

Drew University

College of Liberal Arts

Circulating Tumor Cell Isolation using Immuno-Microbubbles

A Thesis in Biochemistry

by

David Van Dongen

Submitted in Partial Fulfillment of Requirements for the Degree of Bachelor in Arts

With Specialized Honors in Biochemistry

May 2019

Abstract

Cancer has been a constantly escalating threat to human health, affecting millions of people across the globe. In the United States alone, there are nearly 600,000 new cases diagnosed annually, with that number expected to rise in the coming years. Many cancers lack effective treatment methods due to the sheer heterogeneity of cancer diseases, necessitating future medicine to become more personalized. Cancer, at its core, is an accumulation of mutations in one's genetic material that leads to uncontrolled cell growth and division. People naturally accumulate genetic mutations as a result of exposure to carcinogenic substances, as well as by innate mechanisms within DNA replication, meaning that cancer is a disease that is essentially inevitable.

In order to attain a more personalized approach to cancer therapeutics, efficient diagnostic and prognostic tools must be developed such that treatable qualities of the cancer can be identified. Circulating tumor cells (CTCs) have garnered attention in this area in recent decades for their unique role in the metastatic process, as well as their potential to act as a prognostic marker. Unfortunately, CTCs exist in such low quantities in the blood that efficient isolation methods have eluded scientists since their discovery.

These experiments seek to establish an inexpensive and efficient method of CTC isolation using antibody-tagged microbubbles. Microbubbles are small, gas filled, lipid monolayers, which have been used for a variety of theranostic applications for their unique acoustic properties, targeting efficiency, and buoyancy. The system proposed in this study seeks to use immuno-microbubbles to capture CTCs from whole blood samples of cancer patients for their quantification and characterization. To this end, a model of the

system using fluorescently labeled red blood cells (RBCs) was used to verify the potential of this system to capture a small population of cells from the context of a significantly larger population of unlabeled RBCs.

From our experimentation, it was found that around 72% of labeled RBC could be rescued from a much larger population of unlabeled RBC. The linkage between the immuno-microbubbles and the RBC was verified using microscopy. The recovery rate of RBCs matches or exceeds the current gold standard techniques of CTC isolation. This suggests that the use of immuno-microbubbles to isolate CTCs from patient blood samples is a viable and efficient technique.

Table of Contents

Introduction.....	1
Cancer: Impact and Aging.....	1
Cancer: Heterogeneity and Personalized Medicine.....	4
Cancer: Hallmarks and Mechanisms.....	7
Circulating Tumor Cells.....	15
CTC Isolation Techniques.....	19
Microbubbles: Properties and Uses.....	21
Materials and Methods.....	29
Formulation of Microbubbles.....	29
Antibody conjugation to microbubbles.....	30
FITC labeling of RBC.....	31
Capture of FITC-labeled RBC.....	32
Capture of FITC-labeled RBC from unlabeled RBC population.....	32
Microscopy imaging.....	33
Results.....	34
Immuno-microbubble formulation.....	34
Optimization of CTC recovery system.....	36
Initial attempts of RBC-FITC isolation using immunomicrobubbles.....	38
Increasing microbubble size to improve recovery rate.....	39
Rescuing of FITC-labeled RBC from a population of unlabeled cells.....	41
Fluorescence and light microscopy of isolated cells.....	42
Discussion.....	44
References.....	53

Introduction

Cancer: Impact and Aging

Cancer has become one of the most widespread and complex diseases of our time due to the sheer number of people afflicted and the mechanisms by which individuals develop the disease. Based on data from studies completed between 2013 and 2015 by the National Cancer Institute, approximately 38% of men and women will be diagnosed with some form of cancer in their lifetime, with a five year survival rate for some cancers as low as 8%, making it one of the leading causes of death both in the United States and around the world (National Cancer Institute, 2018a; American Cancer Society, 2019). It was estimated that about 1.8 million new cases of cancer would arise within the United States in 2018 alone, in addition to the over 16 million that already live with cancer in some form. Each year, it is expected that we will see over 600,000 deaths in the United States. While enormous progress has been made in the treatment of cancer, it remains the case that fewer than 70% of cancer patients will survive longer five years after initial diagnosis. All of this is despite the nearly \$150 billion spent in the United States to treat those surviving with cancer today. Some estimates have even gone so far as to say that worldwide, the cost of cancer annually is just under a trillion dollars (Cancer Research UK, 2016). These expenses are expected to increase in the coming years. Today, it is rare to find someone whose life has not in some way been touched by cancer afflictions in some capacity.

In general, it seems those most at risk for developing cancer are in our eldest age bracket (National Cancer Institute, 2015). This fact has been confirmed in seemingly

endless epidemiological studies of cancer frequencies (Harding et al., 2012; Pederson et al., 2016). In fact, aging has been described as *the* major carcinogen, since as we age, the development of cancer seems nearly inevitable, as will become apparent based on the mechanism of cancer development (National Cancer Institute, 2018b). As will be discussed in greater detail, cancer, in its simplest form, is an accumulation of mutations that lead to uncontrolled growth and division of cells. Given time, our genes will naturally accumulate mutations, and as more time goes on, more mutations will be garnered by our genes.

There are several reasons accounting for the influence of time on the number of mutations gathered. Perhaps the most intuitive explanation is that we are surrounded by DNA-damaging agents, otherwise known as carcinogens, everywhere we go. The International Agency for Research on Cancer (IARC) has published data over the last 30 years and established that there are exist over 110 substances that are known to be carcinogenic that we may interact with frequently, with hundreds more classified as probably or possibly carcinogenic (American Cancer Society, 2016). To give some perspective, a few of these carcinogenic substances include processed meat, tobacco, alcohol and UV radiation. Though some may find it easy to avoid some of these carcinogens with dietary changes and avoidance of substance use, it is rather difficult to avoid many, such as UV radiation which comes directly from sunlight. While carcinogens do not instantly cause cancer, it does stand to reason that constant interaction with these substances will increase risk as time goes on. Since nearly all of us are

chronically exposed to DNA damaging agents, the link between aging, mutation rates and cancer is fairly well defined.

If mutations are caused from interactions with external and foreign materials that somehow find their way into our DNA and wreak havoc, is it possible to simply live in a bubble and avoid cancer? Unfortunately, the short answer to this question is no.

Mutations rates are inherently encoded within our genes themselves through the infidelity of DNA polymerases, which are responsible for replicating our DNA (Pray, 2008). After all, natural selection would not favor a system incapable of genetic alteration. The role of genetic instability as a result of imperfections in both DNA replication fidelity, as well as the imperfection of DNA repair mechanisms, have long been explored as a key aspect of the development of cancer. Replicative polymerases in eukaryotes make an error once in every 10^4 - 10^5 DNA bases. To add to this, DNA repair machinery is able to recognize and correct about 99% of these mistakes through several complex pathways. Though this seems to be an incredibly high rate of correctness, there is a small amount of room for error. In a human genome of around 6 billion base pairs, even an efficiency this high leads to between 3 and 6 mutations per round of replication. Based on the number of times each day that the cells in a human body replicate, this leads to between 100,000 and 1,000,000 spontaneous lesions each day (Preston et al., 2010). This means that errors in DNA replication account for at least 85% of the mutations in our DNA, making DNA replication even more harmful to our genetic information than external carcinogens.

A 2016 study encompassing data from hundreds of thousands of individuals included in the Danish Cancer Register and from the Danish Cause of Death Register

from between 1978 and 2012 found that this trend of increased age being correlated to increased risk of cancer was valid up to a certain point (Pederson et al., 2016). It was observed that most forms of cancer have a peak prevalence at around 85 years of age, with a decrease in risk after that age. Though this trend is possibly explained as an inherent quality of cancer that makes it less likely to develop cancer once one reaches a very old age, it seems more likely that certain individuals are less inclined to develop cancer and therefore survive longer. If those who develop cancer by age 85 are dying off as a result of the disease, that would leave a population of individuals less likely to develop cancer. What this implies is that there is some either genetic predisposition or some lifestyle and environmental impacts that can act as a preventative measure. Indeed, a great number of studies have been performed to test exactly that, though we are yet to establish a foolproof method of preventing cancer.

As the overall lifespan of humans increases, as is has been for the past century, cancer becomes a bigger and bigger threat to our collective well-being (Roser, 2019). Even with billions of dollars spent on cancer research and care every year, we still only inch towards a solution to the cancer epidemic. This slow progression is simply unacceptable, as cancer is constantly changing and adapting faster than we are advancing.

Cancer: Heterogeneity and Personalized Medicine

In truth, cancer is far more than a single disease, but is rather a collection of complex diseases, with extreme heterogeneity from one case to the next (Dagogo-Jack and Shaw, 2018). It is characterized by an abnormal growth of cellular tissue, with a

tendency to spread to surrounding tissues, and beyond, which in truth, is a rather broad description of a disease. As mentioned, it occurs as a result of an accumulation of mutations that affect a cell's ability to regulate growth and survival, in order to initiate a seemingly limitless replicative potential and effective immortality. Generally, these mutations activate systems that already exist within the cell's genetic code, but are inactivated during normal cellular functions. However, the heterogeneity arises from the specific systems activated or inactivated in specific cancer types, as well as the tissue type affected by the cancerous growth. Given the number of gene mutations with the potential to lead to cancer, it is highly unlikely that any two cancers will be identical.

Since the odds of one person's cancer matching the same genetic profile as another's cancer is extremely low, there is an apparent need for a personalized medical approach. What this means is that the best way to fight cancer is to fight each *specific* cancer, rather than using the same toolset of medications for every disease that is under the blanket term "cancer". After all, each cancer is basically an entirely separate disease from another cancer. Nobody would expect a flu vaccine to prevent malaria. The same principles apply to cancer treatments.

Therefore, it is crucial to consider personalized medicine for the sake of treatment plans for the patient. Each drug on the market works via a unique mechanism of action, and will be most effective against a cancer that has arisen from mutations in genes that are associated with the mechanism of that specific drug. For example, for certain breast cancers, a drug such as doxorubicin may prove a highly chemotherapeutic agent, while as a bladder cancer may be better combated with a drug like cisplatin (National Cancer

Institute, 2019; Li et al., 2019). Nearly all cancer drugs have limited selectivity, meaning that they are potentially damaging to many kinds of cells, beyond simply cancer cells.

This should make sense, since unlike diseases caused by bacteria or viruses, which have defining molecular characteristics distinct from human cells, cancer is made from a patient's own cells, which are often difficult to differentiate from normal cells.

Chemotherapy often has major side effects on cancer patients because of the inefficiency of targeting, which means that receiving the most effective cancer treatment is of paramount importance. Otherwise, the toll of the treatment and the enormous expenses associated with care would be all for nothing.

Recent developments in genetic analysis of tumor cells have greatly improved the ability of the medical community to apply personalized medicine to cancer patients. The knowledge of familial genetic links to cancer, for instance, has provided insights into specific characteristics that an individual's cancer may adopt (Centers for Disease Control and Prevention, 2018). It is relatively common to see that family members share susceptibilities to similar cancers, and while not every facet of genetic predisposition to cancer is understood, the trends in family history provide much needed insight that can lead to personalized care.

Some other advances include that of genomic sequencing and RNA profiling. These techniques have the potential to give invaluable insights into the molecular nature of the tumor (National Cancer Institute, 2017). RNA profiling gives scientists the ability to establish the genes that are being activated, the quantities of their gene products that are produced, and give clues as to the protein profile of the cell. Ultimately, this can lead

to the prescription of medication that can properly combat the set of mutations present in each specific cancer. Unfortunately, as much as these techniques can improve our ability to provide personalized care, there are limitations. For instance, tumors possess inherent heterogeneity, not even simply from one cancer to another, but even within the same tumor. Tumors generally have several smaller populations of cells, each with unique characteristics. This can limit how useful the genotype of any single tumor cell can be, as the individual sequence tells relatively little about the tumor as a whole. Also, the tumor itself is constantly accumulating more mutations, meaning that it is only a matter of time before any genetic information becomes “dated”. Therefore, the most effective way to use these techniques would be to target subpopulations of cells that are most likely to cause damage and have the means to quickly and effectively target those cells.

Cancer: Hallmarks and Mechanisms

In an attempt to connect all cancers under one umbrella set of conditions, a 2000 paper written by Hanahan and Weinberg describes six generalized hallmarks of cancer. These hallmarks include a self-sufficiency of growth signals, evading apoptosis, an insensitivity to anti-growth signals, sustained angiogenesis, limitless replicative potential, and tissue invasion and metastasis (Hanahan and Weinberg, 2000). While each individual hallmark is expected to vary from one cancer to the next, it is these traits that usually lead to cancerous growth. These six hallmarks stood as the unifying themes for all forms of cancer up until recently, when a few more hallmarks were accepted by the scientific community.

It was in 2011 that Hanahan and Weinberg revisited their initial six hallmarks of cancer and established two more “emerging hallmarks”, as well as two “enabling characteristics”(Hanahan and Weinberg, 2011). The former included deregulating cellular energetics and avoiding immune destruction, and the latter including genome instability and mutations, as well as tumor-promoting inflammation. Though these eight hallmarks and characteristics are not without controversy, they have largely been accepted as the defining features of cancer at large.

To fully understand the nature of cancer, it is necessary to comprehend these hallmarks individually with a brief overview of each. Beginning with the first hallmark, cancer cells are able to become self-sufficient in growth signaling through mutations in signaling pathways that are normally activated by diffusible growth factors or transmembrane receptors that are typically activated by surrounding cells. Cancer cells, instead, find ways to sustain these pathways even in the absence of communication from other cells (Schwab, 2011). A classic example of a mutated pathway in cancer that ultimately leads to overgrowth of cancer cells is the Hippo signaling pathway, which regulates cell proliferation and cell death (Soubrier et al., 2018). The name “Hippo” was given to the pathway because uncontrolled signaling can lead to largely oversized tissue or organs in animals.

Normally this growth is also suppressed by surrounding cells, which can secrete anti-growth signals, as an additional mechanism to prevent cancerous growths. It may not come as a surprise, and will be observed as a theme for these hallmarks, but cancer cells are able to accumulate mutations that allow them to ignore these antigrowth signals.

There are several genes and pathways in normal cells, such as p53, PTEN, ARID1A, Notch, and IGF (Ruhul Amin et al., 2015). Though the exact pathways by which these genes operate is beyond the scope of the work completed here, it is important to recognize the sheer variety of genes that may be altered to allow the dysregulation of anti-growth signals. Mutations on any of these tumor suppressor genes, as well as countless more, can lead to a cancer-like state from an overgrowth of cells and tissue.

Typically, cells are able to sense dysfunction in either of these pathways and determine that for the betterment of surrounding cells and tissue, cell death pathways should be activated. The most prominent mechanism of cellular suicide is apoptosis, wherein cells will implement a cascade of special proteases, called caspases, which will break down the interior components of the cells (Alnemri et al., 1996). Cancer cells are able to shut down this pathway, along with other cell death pathways, in order to avoid cell death.

Even after becoming completely independent of cell-to-cell signalling, normal cells possess a seemingly finite replicative capacity. Once a cell has reached this maximum number of divisions, it reaches a state deemed senescence, wherein it is no longer able to undergo the cycle of mitosis. Through further mutations, cancer cells are able to acquire the ability to shut down the regulatory systems in place to prevent replication. For example, studies have demonstrated that disabling two genes, p53 and pRb, is enough to cause a “crisis state”, which allows the cell line to become immortalized and replicate indefinitely (Wright et al., 1989; Sulli et al., 2019).

Tumor cells often survive in a harsh microenvironment, where the standard vasculature is unable to provide necessary components for survival, such as oxygen and nutrients. Typically, the existing vasculature remains relatively quiescent once development is complete, preventing the growth of new blood vessels or even the branching of existing ones (Hanahan and Folkman, 1996; Huang et al., 2013). To circumvent this issue, cancer cells will both secrete factors that seemingly coax new branches of blood vessels to form towards the cells, while also diminishing factors that prevent this growth. The process of new blood vessels forming from existing vasculature is called angiogenesis. This capability is often acquired later within the cancer cycle, but is essential for the tumor to develop beyond a limited size.

Before describing the final of the initial six hallmarks, we will take a brief sojourn in the area of the newer hallmarks, beginning with the capability of tumor cells to evade immune destruction. Under normal conditions, cancerous or potentially cancerous cells are consumed by macrophages within the body to destroy malfunctioning cells. A paper published in 2009 begins to suggest this quality of tumor cells to evade this destruction may arise from an overexpression of surface markers, such as CD47, which are highly expressed in various forms of stem cells (Jaiswal et al., 2009). This overexpression sends a “don’t eat me” signal to surrounding immune cells and prevents phagocytosis from macrophages. This very overexpression was observed in myeloid leukemias, which provided support for the initial claim that it may be involved in the progression of tumorigenesis. Additionally, the transient upregulation of CD47 in mouse stem cells and progenitor cells directly correlated with the likelihood that those cells

would be targeted by macrophages, with higher expression leading to lower targeting. This hallmark continues to be characterized and confirmed, with many genes, such as TGF β being implicated in the development of immune response evasiveness (Tauriello et al., 2018).

Along with the additional oxygen provided to tumor cells from angiogenic capabilities, tumor cells often require further modification of their systems to provide sufficient cellular energy. Tumor cells often find ways to provide energy through a metabolic switch to glycolysis, rather than oxidative phosphorylation, a process known as the Warburg Effect (Zhang et al., 2013). This switch may seem illogical, as glycolysis results in significantly less energy than oxidative phosphorylation. It is still not entirely certain why the Warburg effect occurs, though many papers have been published in order to explain it. The metabolic switch leads to an increase in glucose transport into cells, as well as an increased production of lactate. These qualities may be useful for rapid generation of ATP, despite the overall amount produced, cell signalling through the generation of reactive oxygen species, or it may support biosynthesis necessary for increased cell growth. This metabolic switch is similarly observed under cellular stress conditions, such as hypoxic conditions. Knowing the cell's typical responses to hypoxia provides a logical mechanism by which a tumor cell may acquire the ability to regulate its metabolism to favor a seemingly less efficient method of producing energy (DeBerardinis et al., 2008).

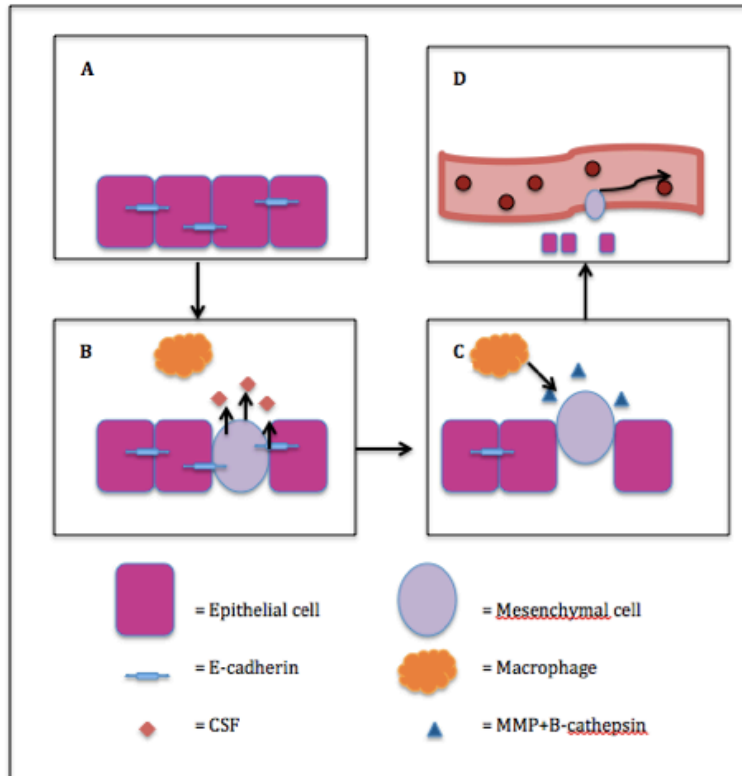
Perhaps the most important of these hallmarks for patient survival is the process of tissue invasion and metastasis. Metastasis is the process of a primary, solid tumor,

developing the ability to migrate into tissue in other regions of the body. It happens as a two phase process, beginning with tumor cells developing the ability to migrate away from the initial tumor site, and ending with the cells becoming capable of surviving in varying tissue environments. While an isolated cancer can be very dangerous for an individual, it is most frequently the seeding of secondary tumors that leads to the eventual death of a patient. For perspective, nearly 90% of females diagnosed with breast cancer survive beyond five years after their diagnosis, while fewer than 27% with metastatic breast cancer survive that long (Seyfried and Huysentruyt, 2013). This is because localized tumors, while they may be detrimental to the immediate vicinity in which they occupy, metastatic cancers can affect many regions of the body and can ultimately cause the failure of multiple organ systems. It has been estimated that over 90% of overall cancer deaths are a direct result of the metastatic process.

Despite our collective knowledge of the dangers of metastasis, much remains unknown about the process itself. For instance, it is very common to observe that cancer in a given tissue will favor another specific tissue for the seeding process (Sartor and de Bono, 2018). For example, prostate cancers tend to favor the bones and lymph nodes for their secondary tumor sites, seemingly with little justification. Additionally, we still lack a definitive answer as to why some cancer cells are able to metastasize and others stay within the primary tumor. This knowledge could prove crucial to our ability to develop effective therapeutics against cancers in the future.

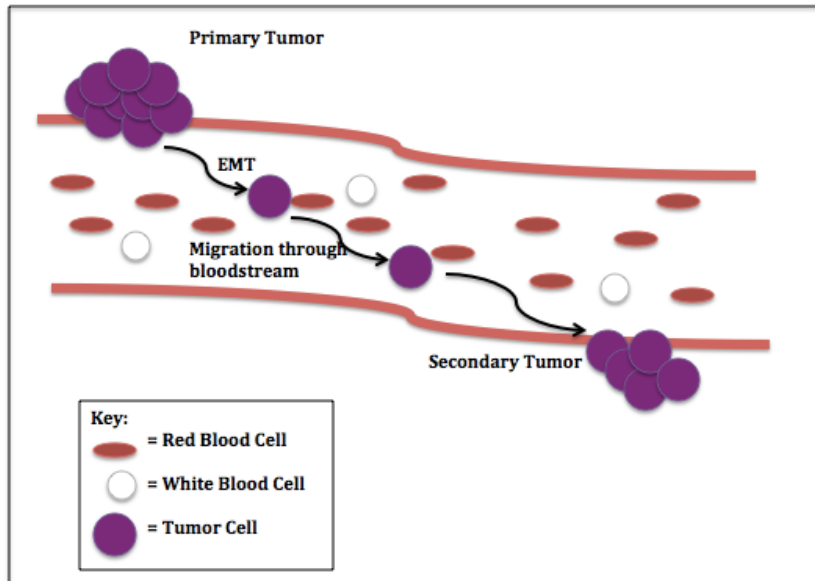
One element of metastasis that is known is how cells can move from a solid tumor state into a circulating tumor state. This process involves the use of the “epithelial to

mesenchymal transition” (EMT). In truth, there are three different variations of EMT, though only type 3, the type that leads to tumor metastasis, will be discussed. The process of EMT is very complex, but can be broken down into a few, more simple steps. To begin, the primary tumor cells possess an epithelial nature, wherein they are stationary and exist within the basal layer of the epithelium tissue which surrounds a blood vessel. In this state, it will possess a genetic profile that consists of the expression of epithelial markers, such as E-cadherin, cytokeratin and many others which are responsible for the anchoring of neighboring cells together and the cytoskeletal rigidity of the cells. From this state, the transcription of these structural elements corresponding to epithelial morphology is diminished through the recruitment of macrophages through the secretion of colony stimulating factor (CSF) (Chen et al., 2017). The macrophages secrete epidermal growth factor (EGF) and tumor necrosis factor- α in order to alter the gene expression profile of the tumor cells, and cathepsin-B, a protease which cleaves the E-cadherin holding the tumor cells in place (Tan et al., 2013). Once the gene expression aligns more closely with migratory cells, the macrophages will secrete matrix metalloproteins (MMP) in order to degrade the basement membrane, leading into the vasculature. The newly altered genetic profile of the now mesenchymal-like cells will promote its permeability into the blood vessels, which ultimately allows their transition into the bloodstream (Model 1).



Model 1. Epithelial to mesenchymal transition (EMT) of tumor cells. (a) The tumor cells adopt an epithelial state, connected by E-Cadherin. (b) Tumor cells alter their gene expression to change their morphology and secrete CSF to attract macrophages. (c) Macrophages secrete cathepsin-B and MMP to cleave E-cadherin and promote the migration away from the endothelium. (d) The mesenchymal tumor cell is able to permeate the vasculature and migrate through the bloodstream.

Once the process of EMT has occurred, the seeding of the secondary tumor may initiate. This process actually requires the reverse of EMT to occur, a mesenchymal to epithelial transition (MET). While many facets of EMT remain a mystery, even less is known about MET. Nonetheless, it is the process of EMT, a subsequent migration of these circulating tumor cells, and the eventual seeding of the secondary tumor that defines metastasis (Model 2).



Model 2. Metastatic process to seed secondary tumors. The process by which a primary tumor metastasizes and leads to a secondary tumor after circulation through the bloodstream.

Circulating Tumor Cells

Despite the ability of some cells to shed away from the primary tumor and circulate through the blood, not all of those tumor cells are capable of metastasizing and seeding secondary tumors. In fact, as few as 0.1% of these “circulating tumor cells” (CTCs), are capable of producing secondary tumors (Krebs et al., 2010). The inefficiency of this process is not entirely understood, and may be related to the MET, as well as immune system interactions with CTCs as they travel through the blood. The CTCs that happen to possess tumor-initiating properties are often referred to as the “decathlon champions” for their superior migratory abilities. It is unclear at this point what differentiates these decathlon champions from other CTCs, though a few ideas have been proposed. In a recent study, CTCs from breast cancer patients were observed to analyze

specific markers present on the CTCs (Theodoropoulos et al., 2010). In particular, CD44, CD24 and ALDH1 phenotypes were assessed because of their inherent similarity to stem cell progenitors, which has been theorized to increase the likeness of seeding by CTCs. Further studies have attempted to correlate these markers to CTCs found in patients with metastases, which has yielded support to the claim that stem cell properties are necessary for secondary tumor formation from CTCs (Bacelli et al., 2013).

The reason for cancer stem cells having the capability to seed better than typical mesenchymal cells has not been demonstrated, though it does make conceptual sense. Stem cells possess more neutral biomarkers which prevent recognition by the immune system and thereby prevent the destruction of CTCs. Additionally, the more plastic properties of the cells may provide beneficial versatility when seeding in a new microenvironment. Despite these seemingly plausible hypotheses, further research is needed to establish a full theory of why certain CTCs possess seeding potential, while other do not.

Even though only a fraction of CTCs that are decathlon champions are capable of causing metastasis, one may wonder why metastasis remains at bay for as long as it does in cancer patients. It can take months or years for certain kinds of cancer to metastasize, despite already having CTCs present and circulating through the blood (Ye et al., 2017). This delay in metastasis is primarily the result of the sheer infrequency of CTCs within the blood. A 2011 meta-analysis, incorporating data from four studies aimed at comparing the number of CTCs to patient prognosis in prostate cancer patients completed over that last 15 years, demonstrated that having approximately 5 or greater CTCs in 7.5

mL of blood was correlated to a poor prognosis and eventual metastasis (Wang et al., 2011). This means that at any one time, there exists an extremely low number of these cells, even in cases where an individual is on the verge of metastasis.

As demonstrated in this same study, the number of CTCs in the peripheral blood of prostate cancer patients appears to have a correlation to the patient prognosis. In general, the more CTCs that can be found within the blood, the worse the outcome for the patient. The number and qualities of CTCs in the blood has a direct relationship with the rate of metastasis, as well (Markiewicz et al., 2014; Aceto et al., 2014). Even though only a small number of CTCs are decathlon champions, having more of them increases the chance of metastasis occurring. The implications of this trend are that CTCs and their collection from the blood can provide immensely useful information about the stage of an individual's cancer. This provides a basis for using CTCs as a method to determine personalized medical approaches to a specific cancer patient.

While the ability to collect and quantify CTCs is powerful in and of itself, CTCs can provide even more valuable information using more modern technology. For instance, single cell RNA sequencing holds the potential to determine the gene expression profile of CTCs, and by extension, much of the genetic profile of the primary tumor (Zhu et al., 2017). Beyond even the analysis of mRNA within a cell to determine the transcriptional profile, single cell RNA sequencing methods possess the ability to determine the types of microRNAs and tRNAs, which can affect the protein expression of a cell, and nucleolar RNAs, which are capable of controlling the RNase capability of a cell. Though the limitations of this technique, such as the mutation rates of cancer and

the heterogeneity of tumor cells, have already been discussed, CTCs may act as a unique cell type for this personalized medicine approach. This is because we already have evidence that it is these cells that are leading the most deadly aspect of cancer, metastasis. Therefore, treatment of the genetic mutations of these cell types stand the best chance of providing a positive outcome for the patient.

This has already been accomplished to identify the expression profile of extracellular matrix proteins of pancreatic circulating tumor cells (Ting et al., 2014). The study was completed using the well established RNA-seq strategy, which entails using the RNA isolated from the cytoplasm to make a library of complementary DNA fragments which can each be tagged and then analyzed through sequencing and comparison to known genomic information. This will be able to qualitatively determine the genes that have been transcribed, as well as quantitatively determine the amount of expression based on the number of reads of a specific RNA fragment. This allows the generation of “heat maps” that describe the expression levels of the genomic information. In this 2014 study, the genetic profile of CTCs captured shed light on crucial aspects of the metastatic process through comparison of the CTC transcriptional products to that of the primary tumor. Because of the information gathered from CTCs, new medicinal targets were able to be identified which may be pertinent to the metastatic process, which as discussed previously, is the major cause of death from cancer.

CTC Isolation Techniques

Since CTCs are so rare within the blood, it can be very difficult to actually capture and analyze them. According to some estimates, although one would not find greater than 10 CTC within a mL of blood, there are more than a million white blood cells and well over a billion red blood cells (Haber and Velculescu, 2014). This signal-to-noise ratio is astronomical, and consequently requires extremely sensitive isolation techniques to differentiate between CTCs and blood cells. Because of this challenge, a number of creative solutions to CTC isolation have been developed and tested. For example, many forms of microfluidics, using size based isolation or magnetophoresis, density-based separations, and immunomagnetic bead separation have all been employed to attempt CTC isolation (Zhang et al., 2017; Karabacak et al., 2014; Hosokawa et al., 2013; Kermanshah et al., 2018). Each of these techniques have demonstrated promise, but each also has its shortcomings. The only method of CTC isolation currently approved by the FDA is an immunomagnetic separation technique called CellSearch (Muller et al., 2012).

CellSearch is an assay that was first developed in 2000, and quickly became the gold standard in CTC isolation (Reiter et al., 1998). It is a method that relies on the presence of biomarkers on the CTCs and targets those markers using ferrofluid nanoparticles that are coated with antibodies for those biomarkers, namely the Epithelial Cell Adhesion Marker (EpCAM) (CellSearch Circulating Tumor Cell Test, 2019). These CTCs are directly rescued from a 7.5 mL blood sample from patients. Once they have been removed from the blood sample, cells are stained with anti-CD45 antibodies to

fluorescently label any leukocytes that may have been captured, as well as anti-cytokeratin antibodies, which fluorescently label epithelial-like cells. The cells that have been captured can then be counted using fluorescent microscopy, since any noise captured by the magnetic separation can be discarded upon visual inspection of the cells.

While this technique has been largely successful, it has also been scrutinized for many qualities that limit its applicability (Wang et al., 2017). For instance, positive enrichment methods generally rely upon the presence of specific biomarkers on the surface of the CTCs, which may exclude cells that do not have these markers present. While it is true that many CTCs express EpCAM, early phase patients has demonstrated a decreased expression, with only between 20%-40% of CTCs within their blood possessing this marker. The inherent heterogeneity of cancer prohibits reliance on a single marker for all CTCs. Additionally, the process of immunomagnetic separation has the potential to damage the membrane of targeted cells by imposing too much magnetic force on the cells (Zhang et al., 2016). Given the extremely low quantity of cells that are even able to be captured to begin with, it is crucial to have a methodology that gently rescues that CTCs.

Perhaps the most important critique of the CellSearch system is the price. CellSearch CTC profiling can cost patients thousands of dollars, and the use of the system for research purposes is even more expensive. A single CellSearch kit can cost over \$4000, and the machinery to perform the assays themselves costs more than \$100,000. Without the machinery, one can send out samples to have other facilities perform the tests, which will incur its own expenses, as well as adding excess time to the

process. This makes the technique ultimately impractical and inaccessible to the broader scientific community.

One technique that has attempted to rectify some of these shortcomings of CellSearch is the use of size-based microfluidics. Though there are several variations of this method, one very common way to accomplish size-based separation is the use of isolation by size of epithelial tumor cells (ISET) (Hosokawa et al., 2013). This technique takes advantage of the fact that tumor cells are relatively large compared to leukocytes, and significantly larger than red blood cells. By flowing a blood sample through miniaturized microcavity array (MCA), which is essentially a porous plate that exclude large cells, the CTCs can be isolated from the rest of the blood contents since they will not flow through the pores. The data from this study provided rather inconclusive results, as they were essentially comparing whether patients were found to be “CTC positive” based on if CTCs could be detected using their MCA system compared to CellSearch. They had several positive hits that were unable to be recorded from CellSearch, which could imply an improvement in detection from the CellSearch system, but could also mean a greater chance of false positives. Similar studies comparing ISET techniques with CellSearch have found that CellSearch is generally more reliable, although certain cancers with decreased levels of EpCAM may be better suited to ISET isolation.

Microbubbles: Properties and Uses

Though perhaps an unexpected hero in this story, a possible solution to the issue of rare CTC isolation may lie within the tiny, but mighty microbubbles. Microbubbles are

an incredibly versatile theranostic agent, capable of being used for a large variety of biomedical applications. Fortunately for the sake of explanation, the concept of what constitutes a microbubble is very straightforward based on the name alone: they are tiny bubbles. More specifically, microbubbles are shells made of lipids, proteins or other polymers with a gaseous core that exist on the micrometer scale, usually between 0.5 μm and 10 μm (Sirsi and Borden, 2009). The only limit to the composition of the microbubbles is what can surround and stabilize the gaseous core. On this small of a scale, gaseous bubbles are naturally unstable from surface tension effects, which necessitates a relatively stable shell in order to keep the microbubbles in one piece (Park et al., 2001).

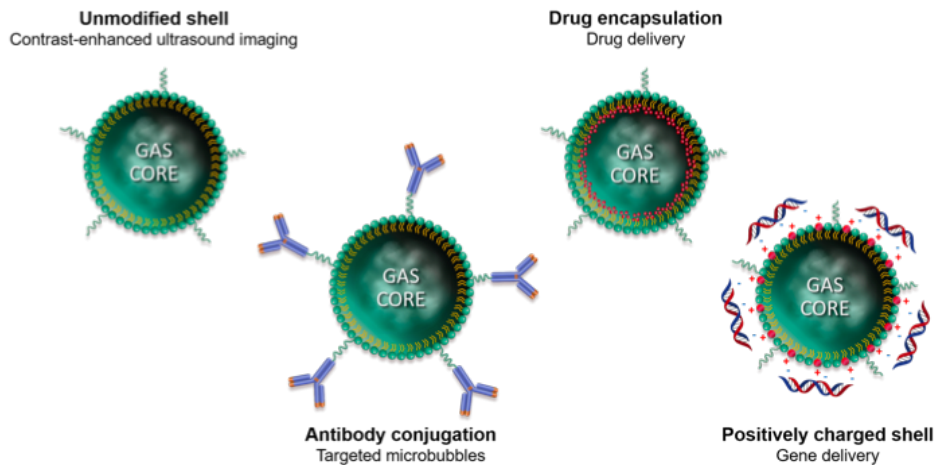
The idea for the creation of lipid coated microbubbles actually originated from similar phenomena in oceans and freshwater, as glycoproteins and acyl lipids spontaneously form small lipid micellar gas bubbles (D'arrigo, 2011). It is the lipid coated microbubbles that are the most ubiquitous within the biomedical field, as they are incredibly easy to create, are made from inexpensive components and can have a large number of macromolecules incorporated into the shell (Sirsi and Borden, 2009). Phospholipids have both hydrophobic and hydrophilic ends, which will spontaneously arrange into monolayers around a strongly nonpolar gas when in an aqueous solution. Consequently, the flowing of nonpolar gas, often perfluorocarbon gas, into an aqueous, phospholipid containing solution will naturally create microbubbles.

Microbubbles possess several useful properties that aid in their overall versatility, many of which can be tuned by modification of the outer shell. For example, microbubble

formulations can be made to be more or less stable based on the intermolecular forces that hold together the shell (Borden et al., 2005). This can be useful in order to control the destruction of the bubbles, which is a necessary step in many microbubble applications, as will be seen. Additionally, the elastic surface and internal pressure of microbubbles make them fantastic contrast agents for ultrasound imaging. This is accomplished because upon interactions with ultrasound waves, pressure changes are exerted upon the bubbles, which makes them resonate at high frequencies that are easily detected by ultrasound machines. This creates a much sharper image than would be seen without the presence of microbubbles. Another useful property of microbubbles is not dissimilar to a property of any bubble that one might imagine: buoyancy. Microbubbles are inherently less dense than their aqueous surroundings which causes a very large buoyant force to be exerted on the bubbles, making them capable of carrying heavy loads. This property will be of particular value to the experiments carried out within this study.

It is because of these properties that microbubbles are used in such a large variety of experiments. Microbubbles have been used as ultrasound contrast agents, drug delivery systems, biomarker targeting agents, gene editing platforms, and even used in tandem with ultrasound to aid in the crossing of the blood brain barrier, a recent feat that has opened the door for much needed therapeutics to be able to enter the central nervous system (O'Reilly and Hynynen, 2018). Their use has even lead to effective therapies for diseases like acute thrombosis, which can quickly be translated into the clinic and improve patient outcomes (Lux et al., 2017). Since the microbubble itself is simply a

scaffold for scientists to manipulate, the possibilities of what microbubbles can be used for is seemingly endless, as noted in Model 3.



Model 3. Variations of microbubbles for a variety of purposes.

Perhaps the most common use of microbubbles that one encounters when sifting through the literature is an ultrasound contrast agent. However, this purpose has been expanded in recent years to give them a far greater purpose. By allowing the amalgamation process to incorporate ligands within the lipid monolayer of microbubble formulations, microbubbles have been demonstrated to have efficient use in ultrasound imaging of specific targeted regions, thereby further enhancing the image of specific targets (Unnikrishnan et al., 2018). Using a mouse adenocarcinoma model, these ligand-coated antibodies were able to target and dramatically improve the image of the mouse tumors with ultrasound. The duration of the signal was nearly 4-fold greater than the untargeted imaging, due to the fact that the microbubbles localized on the area of interest. While this validates the use of microbubbles in aiding the diagnostic aspect of cancer, it is far from the only use in combating the disease.

The use of microbubbles as drug delivery systems is not an entirely new concept, as it originated decades ago, but several new potential therapies are still in development today (Kelly, 1981; Roovers, 2019). In 2017, a study was performed that focused on the use of albumin-based microbubbles coated with cetuximab for the purpose of combating carcinoma (Narihira et al., 2017). Cetuximab is a potent, apoptosis-inducing agent that when introduced to cancer cells, will trigger cell death. The delivery system, in short, functions by allowing the microbubble formulation to enter the bloodstream and performing a focused ultrasound irradiation at the specific tumor afflicted site. The drug that coats the surface of the bubbles is unable to interact with its surroundings due to the interactions with the proteins on the microbubble surface. Once the ultrasound is delivered, the microbubbles burst and release the drug cargo into the surroundings, thereby enabling a targeted therapy. This has resulted in as much as a fivefold increase of carcinoma cells, far exceeding the amount of cancer cell death observed from an untargeted approach.

One of the most groundbreaking uses of microbubbles is their ability to assist in the permeation of the blood brain barrier. Focused, pulsed ultrasound, with the aid of ingested microbubbles, have demonstrated the ability to open the blood brain barrier and allow the passage of therapeutics for several complex central nervous system diseases, including glioblastoma and Alzheimer's disease (Carpentier et al., 2016; Lipsman et al., 2018). This approach has been moved into clinical trials and demonstrated a high degree of tolerance by the patients involved, potentially providing a solution to a decades old problem of membrane permeation. It is because of the blood brain barrier that

glioblastoma remains one of the most difficult cancers to remove; yet again microbubbles have demonstrated the power to overcome this obstacle.

Clearly, microbubbles have proven a worthy adversary for the fight against cancer, particularly against primary tumors, but as discussed, the larger issue lies in the migration of primary tumor cells to secondary locations. Perhaps unsurprisingly, microbubbles have shown potential to target the metastatic phase of cancer as well (Tu et al., 2018). The process of ultrasound mediated microbubble destruction (UMMD) has been developed for gene delivery systems that are capable of enhancing the effects of the immune response to cells that display metastatic potential while circulating through the blood. Genes are delivered to the antigen-presenting tumor cells with high efficiency in order to increase their gene expression of markers visible to immune cells within the blood. This increases the potential for the immune system to eradicate the metastatic cells and decrease the cancer's overall ability to seed secondary tumors.

Microbubbles: a novel method for CTC isolation

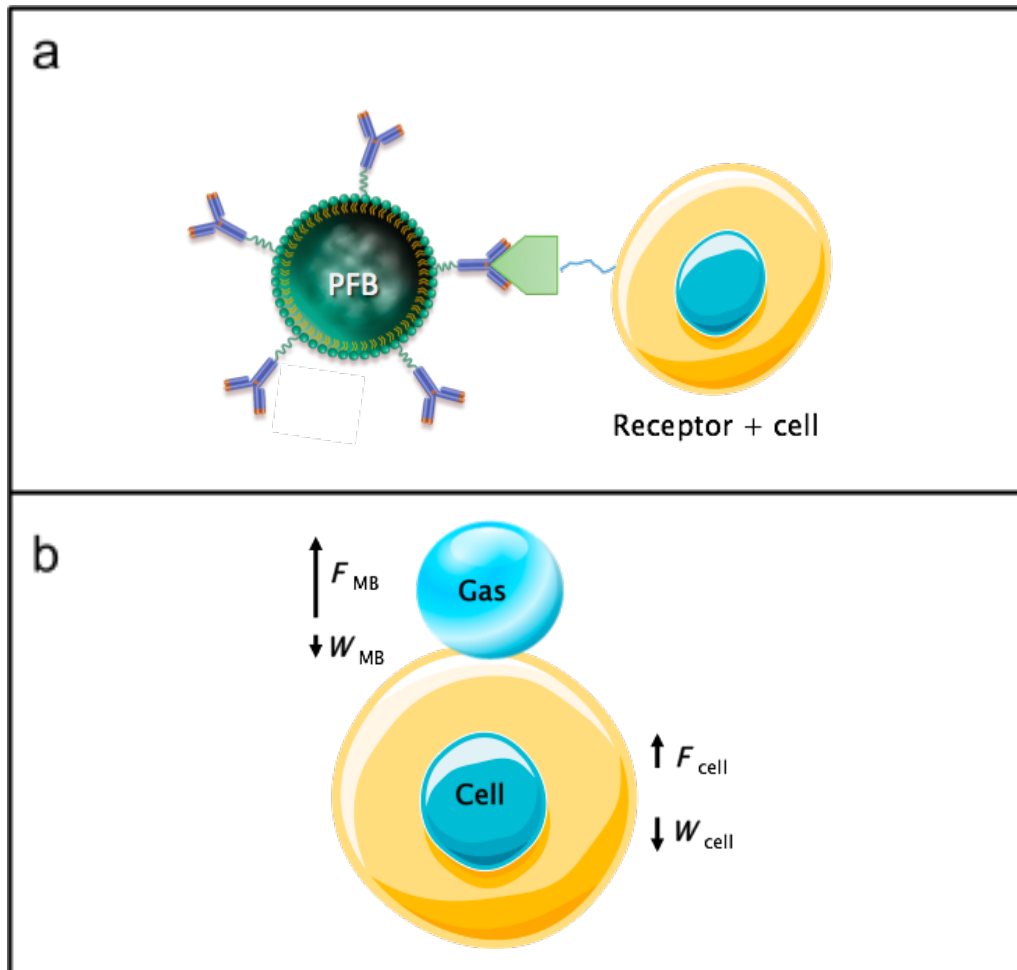
Given the urgent need for methods to determine personalized medical approaches to cancer therapy and the potential insights that CTCs can provide in this capacity, new and more efficient methods of CTC isolation is a necessary next step in cancer therapy. The current methods of CTC isolation, while useful, lack the sensitivity necessary to recover such a small quantity of CTCs from patient blood samples. Microbubbles, through their incredible versatility and ease of use, may provide a unique, efficient and inexpensive method to accomplish this goal.

The system proposed and explored in these experiments is depicted below in Model 4. Lipid-shell microbubbles coated with antibodies, deemed immuno-microbubbles, already exist and could be used for the purpose of targeting CTCs from patient blood samples. By using antibodies specific for biomarkers present on CTCs, such as EpCAM or EGFR, the buoyancy of the microbubbles may be able to enrich the population of CTCs from the blood, thereby making them usable for genetic profiling or prognosis determination.

Prior studies have proposed similar systems, but failed to demonstrate the potential efficiency of the use of microbubbles to rescue circulating tumor cells (Wang et al., 2018). This may be due to a variety of factors, including the methods of detecting the cells that have been captured, the inability to efficiently target the CTCs or perhaps the physical limitations of the microbubbles themselves and the buoyant force that they impose upon the circulating tumor cells. Typical systems use fluorescent microscopy for quantification and target a single antigen that may not be present on every CTC, which may prevent accurate quantification.

In order to explore the viability of this system, RBC labeled with a fluorescent tag, FITC, were used as a surrogate for CTCs and immuno-microbubbles specific for the FITC marker were formulated to target the FITC-labeled RBC (Model 4). The success of the immuno-microbubble formulation was tested using flow cytometry, followed by the optimization of the centrifugation conditions to pellet the cells and allow only immuno-microbubble linked cells to float. The optimized system was tested to confirm the isolation of rare labeled cells, and further improvements were attempted. We

hypothesized that this proposed system could improve the recovery rates observed by current CTC isolation methods and therefore act as a more efficient means of using CTCs for personalized medicine in the future.



Model 4. Proposed method of rare cell isolation using immuno-microbubbles. (a) Using antibody-coated microbubbles, a receptor on a specific cell can be targeted and a linkage formed between the two. **(b)** The buoyant force of microbubble, which will be linked through the antibodies coating the surface, can overcome the gravitational force that would typically either carry the cell to the bottom of a solution, or allow it to be suspended within solution.

Materials and Methods

Formulation of Microbubbles

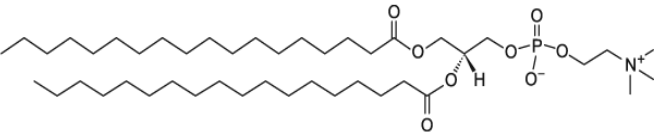
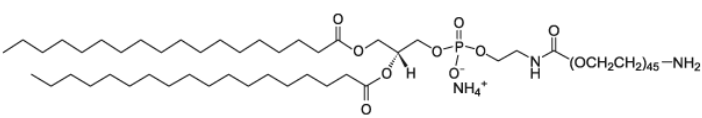
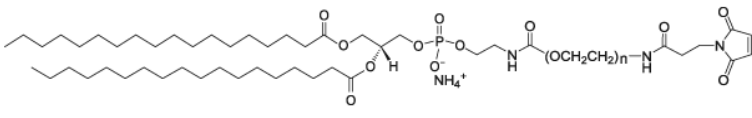
Microbubble formulations were made from lipid films containing 1,2-distearoyl-sn-glycero-3-phosphocholine (DSPC), 1,2-distearoyl-sn-glycero-3-phosphoethanolamine (DSPE) linked to polyethylene glycol (PEG), and DSPE-PEG5k linked to maleimide groups, in a molar ratio of 90:8:2, respectively (Table 1). The lipid films were solvated using in a mixture of PBS 1X/propylene glycol/glycerol (80:10:10 v/v/v) using a total of 2 mL volume. Sonication and heat were used to ensure full solvation of the lipid films.

Amalgamation of the microbubble formulation was completed in sealed vials using a gas exchange of perfluorobutane into the lipid solution. Once the gas exchange was complete, excess pressure was released from the vial using a syringe and the vial was vigorously shaken for a full minute to allow microbubble formation. Microbubble formulations were then washed with three successive rounds of low-speed centrifugation at 300 x g for 3 minutes each. The centrifugation separated microbubbles within the range of 1-6 μm from microbubbles of smaller size (Feshitan et al., 2009). Microbubbles of undesired size were removed and replaced with PBS 1X at pH 6.5 + 1mM Ethylenediaminetetraacetic acid (EDTA), until all washes were completed. Upon the final wash, excess buffer was removed to leave a concentrated sample of microbubbles in the desired size range.

Microbubbles were characterized using a Multisizer to determine the average size and concentration of the microbubble sample. Three successive runs on the Multisizer

were completed in order to confirm the results and the average of the three runs was used to determine concentration and size (Figure 1a).

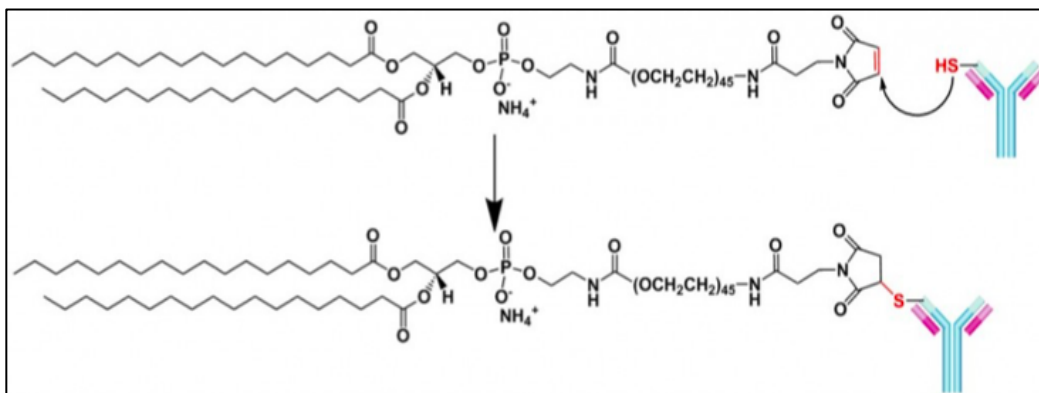
Table 1. Lipid content of microbubble formulations.

Lipid	Structure	Molar Ratio
DSPC		90
DSPE-PEG2k		8
DSPE-PEG5k-Mal		2

Antibody conjugation to microbubbles

Alexa Fluor 488 anti-FITC antibodies were purchased and used to create immuno-microbubbles. Thiolation of the antibodies was completed from incubation of the antibodies with 2-aminothiolane, otherwise known as Traut's reagent, which attaches a reactive thiol group to the surface of the antibodies. Incubation lasted approximately 1 hour, while rotating the sample within a microcentrifuge tube. The resulting thiolated antibody was used to conjugate to the microbubbles through a thioether linkage to the maleimide groups on the surface of the microbubbles from the DSPE-PEG5k-Maleimide

lipids. Conjugation occurred from incubation of the thiolated antibody with the microbubbles for at least 3 hours while mixing (Model 5).



Model 5. Conjugation of thiolated antibody to maleimide groups on DSPE-PEG5k-Mal lipids

Success of the antibody conjugation determined by flow cytometry under four conditions: unconjugated microbubbles, unconjugated microbubbles with secondary antibody (IgG) for fluorescent detection, conjugated microbubbles, and conjugated microbubbles with IgG. Only conjugated microbubbles with IgG should fluoresce in high yield under these conditions, which confirms successful conjugation.

FITC labeling of RBC

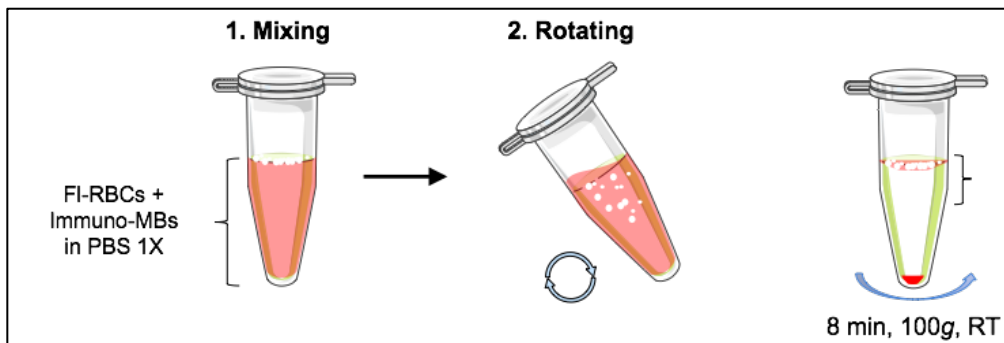
RBC were isolated from whole blood samples acquired from rats. The RBC were purified using centrifugation, since RBC pellet at slower centrifugation speeds than the larger blood contents, such as leukocytes. The supernatant was removed and the remaining blood cells brought up in 1 mL of Hank's Balanced Salt Solution (HBSS). The cells were stored at 0°C.

Fluorescein isothiocyanate (FITC) was prepared using dilution of solid FITC in HBSS buffer to produce a final concentration of 30 μM. The final solution was mixed for

an hour while covered to prevent exposure to light. The FITC solution was mixed with the RBC to label the RBC and the solution was mixed for a total of 3 hours.

Capture of FITC-labeled RBC

The isolation of FITC-labeled RBC was accomplished from mixing and incubation with immuno-microbubbles. This incubation was allowed to persist while rotating for approximately 1 hour to allow efficient linkage between the antibodies and the FITC. Once the linkage was allowed sufficient time to occur, the solution was centrifuged for 8 minutes at 100 x g in order to produce a pellet of RBC at the bottom of the tube. This time and force was established from optimization experiments, seen later in these experiments (Figure 2 and Figure 3). FITC-labeled RBC were quantified by removal of the top layer of the resulting solution, while leaving the cell pellet in tact (Scheme 1). The solution was analyzed and quantified using flow cytometry.



Scheme 1. Capture of FITC-labeled RBC from solution.

Capture of FITC-labeled RBC from unlabeled RBC population

FITC-labeled RBC were placed in the context of a much larger population of unlabeled RBC in order to mimic whole blood patient samples, using approximately

20,000 FITC-labeled cells in 1,000,000 unlabeled RBC. Once the FITC-labeled RBC were mixed, immuno-microbubbles were added to the mixture and the remaining procedure was followed as in Scheme 1. Quantification was completed using the cell pellet to determine the number of FITC-labeled RBC that had not been captured using the immuno-microbubbles, due to the limitations of the flow cytometer set up. The number of FITC-labeled RBC was back-calculated from this quantity.

Microscopy imaging

Microscopy images were taken using a light field microscope (LFM). Images were taken using the capture methods described above with a few changes. First, the immuno-microbubbles used contained a DiD dye in order to visualize the microbubbles under the fluorescence filter. Second, rather than quantification using the flow cytometer, the top layer of the solution was transferred to a slide for microscopy imaging.

Results

Immuno-microbubble formulation

Microbubbles were formulated as described previously. A representative sample of microbubbles can be observed from the multisizer data in Figure 1a. The mean size and concentration of the sample are displayed within the inset of Figure 1a. As the name suggests, the microbubbles are generally within the size range of around 1 to 2 microns in size and a standard concentration of over 1×10^9 microbubbles/mL.

The success of the conjugation of the anti-FITC antibodies was determined using flow cytometry (Figure 1b). The snake-like pattern observed in the region of interest (ROI) of the non-gated plots is a typical signature of microbubbles flowing through the detector. The intensity of the signal corresponds to the number of counts within that ROI. The gated plots distinguish between non-conjugated microbubbles and conjugated microbubbles. Anything to the right of the red line on those plots should have a fluorescence marker, while the count on the right of that border corresponds to anything without fluorescence. The four conditions tested included the control microbubbles (Control MBs) both alone and in the presence of the IgG, and the antibody conjugated microbubbles (immuno-MBs) both alone and in the presence of the IgG. In this representative example, only the condition in which antibody conjugated microbubbles were in the presence of the IgG displayed significant fluorescence. It should be noted that the concentration of the immuno-microbubbles is far below that of the microbubbles alone, as the conjugation process itself results in a loss of microbubbles (Figure 1). A small population of control microbubbles also fluoresced, which was unexpected,

however other experiments did not demonstrate this same small population of cells, so this group was deemed negligible.

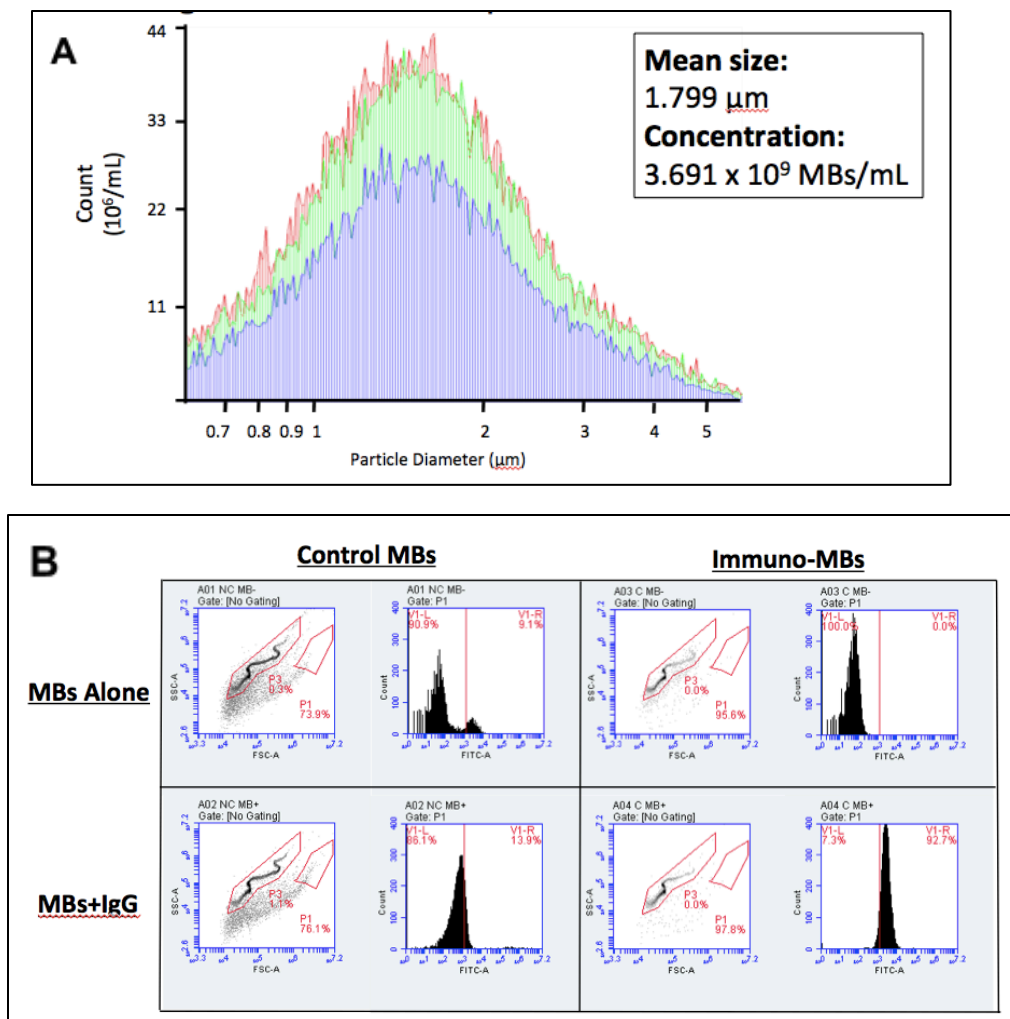


Figure 1. Formulation of immuno-microbubbles. (A) Size of microbubbles in a representative population from one formulation, as measured by multisizer. **(B)** Microbubbles in four conditions were tested both in the non-gated channel and the ROI-gated channel to establish antibody conjugation efficiency using flow cytometry. Four conditions were tested for changes in fluorescence, unconjugated microbubbles alone (top left), unconjugated microbubble with IgG (bottom left), antibody conjugated microbubbles alone (top right), and antibody conjugated microbubbles with IgG (bottom right). Percentage of the count above the threshold fluorescence is displayed on the graphs.

Optimization of CTC recovery system

In order to optimize the proposed system, red blood cells (RBC) were brought up in HBSS in the absence of microbubbles and centrifuged for varying lengths of time to attempt to reduce the number of false positives from unlabeled RBC that manage to remain in the top layer of the solution after centrifugation (Figure 2). These values were normalized to the RBC found in the cream without centrifugation. As the amount of time centrifuged was increased, fewer RBC remained within the cream. Once the centrifugation time was increased to about 8 minutes, little to no RBC could be isolated from the cream. Because of these results, 8 minute centrifugation times were selected as optimal for the subsequent experiments.

Additionally, the centrifugal force was varied to determine the optimal force to pellet the cells at the bottom of the tube and prevent false positives during RBC isolation using immuno-microbubbles (Figure 3). The experiments were performed at 8 minutes, according to the results of the prior experiments. There was an observable steep drop off in the recovery of RBC even at 100 x g, which implied that this force would be sufficient to eliminate false positives during experimentation. In general, lower centrifugal forces are favorable for the RBC, since larger forces may disrupt the cell membranes and cause damage.

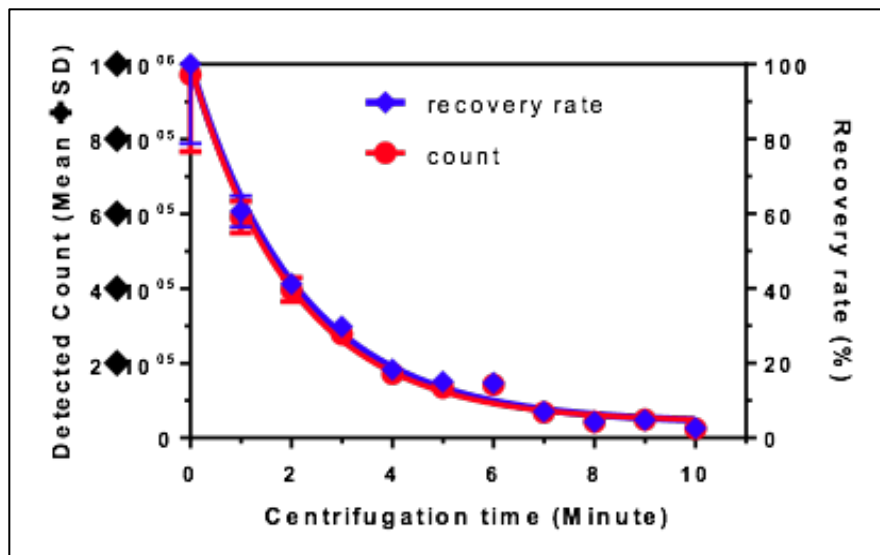


Figure 2. Optimization of centrifugation time to eliminate false positives. RBC collected from the top layer of the solution after varying centrifugation times between 0 and 10 minutes. The standardized recovery rate (blue) and the number of RBC (red) were determined using flow cytometry. *note: \blacklozenge =multiplication.

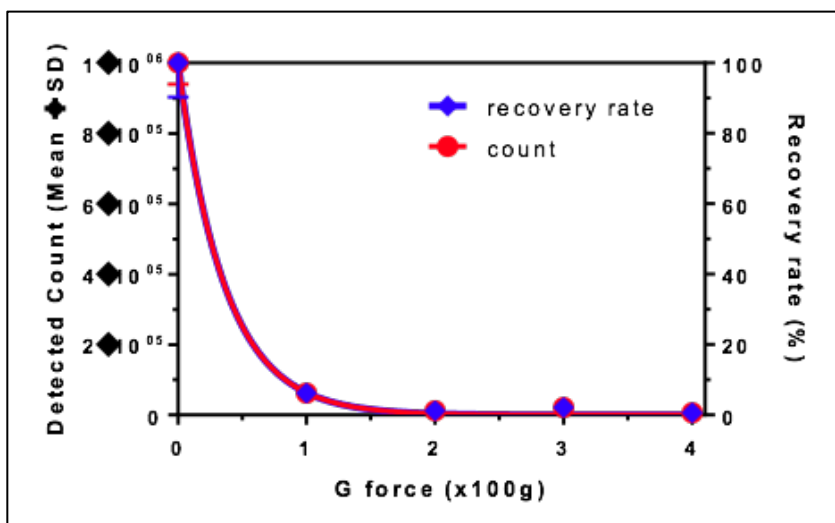


Figure 3. Optimization of centrifugal force to eliminate false positives. The count (red) and recovery rate (blue) determined from varying the force between 0 and 400 x g. *note: \blacklozenge =multiplication.

Initial attempts of RBC-FITC isolation using immunobubbles

Using the optimized system described above, the isolation of FITC-labeled RBC was attempted (Figure 4). Flow cytometry works by flowing a sample through a nozzle in order to allow cells to be counted as they cross multiple laser light sources. The lasers will be able to determine the general size and fluorescence of the cells that pass through. In Figure 4, the axes in the first panel correspond to the forward scattering (FSC-A) and side scattering (SSC-A) of the light as the sample passes through. The P6 ROI corresponds to the immuno-microbubbles linked to RBC, while the P8 ROI represents the microbubbles that were not linked to any RBC. The following two panels correspond to the P6 gated region to establish the amount of FITC-RBC rescued using this method. The fluorescent FITC-A gate is used to measure the fluorescence in the following panel, allowing the establishment of quantification of FITC-labeled cells. The final panel counts the number of cells that crossed the threshold fluorescence gate. The total count found from the final panel corresponded to a 39.5% recovery rate of the labeled RBC, since 19,766 were rescued of the 50,000 that were put in solution. Though this represents a relatively low recovery rate, it does provide promising evidence that immuno-microbubbles may be able to rescue CTCs from patient blood samples.

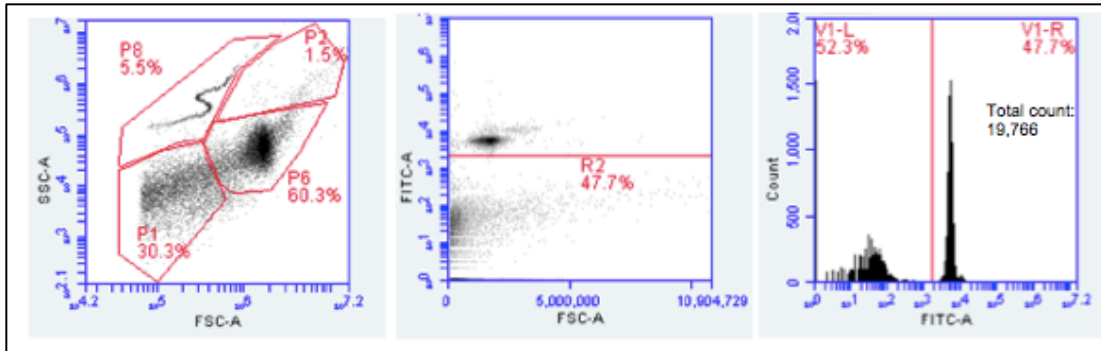


Figure 4. Recovery of FITC-labeled RBC using immuno-microbubbles. FITC-labeled RBC rescued by immuno-microbubbles as measured by flow cytometry.

Increasing microbubble size to improve recovery rate

The size of the microbubbles may have an impact on the efficiency of the recovery of FITC-labeled RBC. It stands to reason that larger microbubbles would be able to exert a larger buoyant force on the RBC. This may result more RBC lifted from the pellet and an increased recovery rate. Following this theory, an attempt to make larger microbubbles was made using differential centrifugation, as described above. The results are displayed in Figure 5 and demonstrate approximately a two-fold increase in the average size of microbubbles.

The larger microbubble formulation was conjugated to anti-FITC antibodies and used to rescue a population of FITC-labeled RBC (Figure 6). The recovery rates determined from this experiment demonstrated a minimal increase in average percentage of cells rescued with no statistically significant difference observed. Normal microbubble populations, therefore, were used for the subsequent experiments.

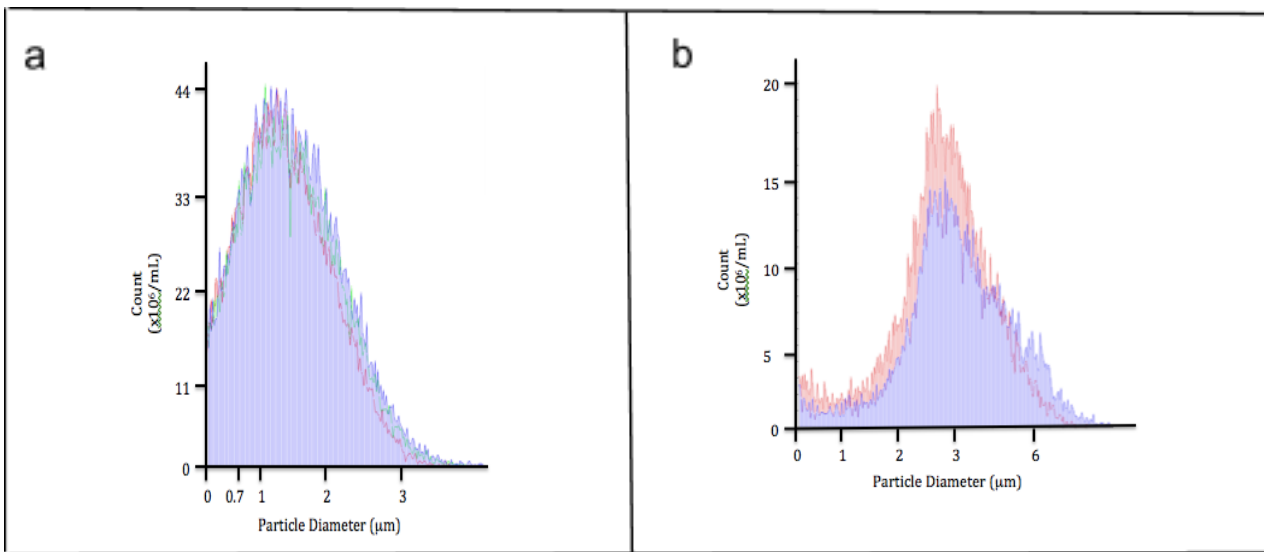


Figure 5. Larger microbubble formulation. Microbubble formulations as measured by multisizer. (a) Normal microbubble formulation. (b) Larger microbubbles retrieved by differential centrifugation.

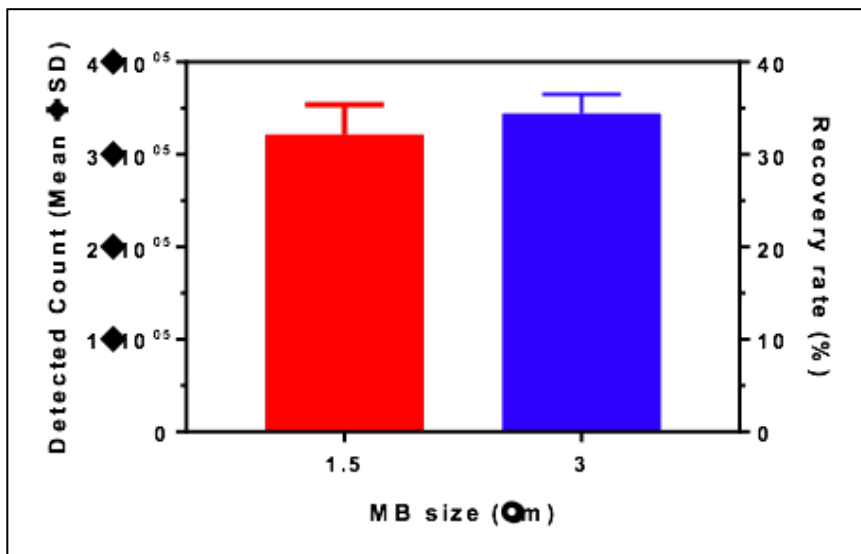


Figure 6. Recovery rate of FITC-labeled RBC using normal and larger microbubble formulations. Percentage of cells rescued as determined by flow cytometry for both the normal (red) and larger (blue) immuno-microbubbles. *note: \blacklozenge =multiplication.

Rescuing of FITC-labeled RBC from a population of unlabeled cells

The ultimate goal of these experiments is to capture cells from whole blood samples from patients. To that end, it is necessary to demonstrate that this system is capable of isolated FITC-labeled RBC from a population of unlabeled cells (Figure 7). Due to the limitations of the flow cytometer, the number of FITC-labeled RBC floated to the top of the solution was back-calculated from the amount of FITC-labeled RBC in the pellet. This was done because the flow cytometer probe counts cells from the bottom of the solution being sampled. Since the microbubbles, in theory, capture cells and float them to the top of the solution, it is likely that the previous measurements of recovery rate were low because the cells floated before the flow cytometer could measure them. As predicted, the amount of FITC-labeled RBC that could be found in the pellet corresponded to 28% of the total number input into the mixture, implying that 72% of the FITC-labeled RBC had floated as a result of attachment to the immuno-microbubbles. As expected, the characteristic microbubble signal in the P8 ROI was unobservable since the microbubbles should not be found in the pellet of the solution. The vast majority of cells counted were unlabeled RBC, with a small population of FITC-labeled RBC present.

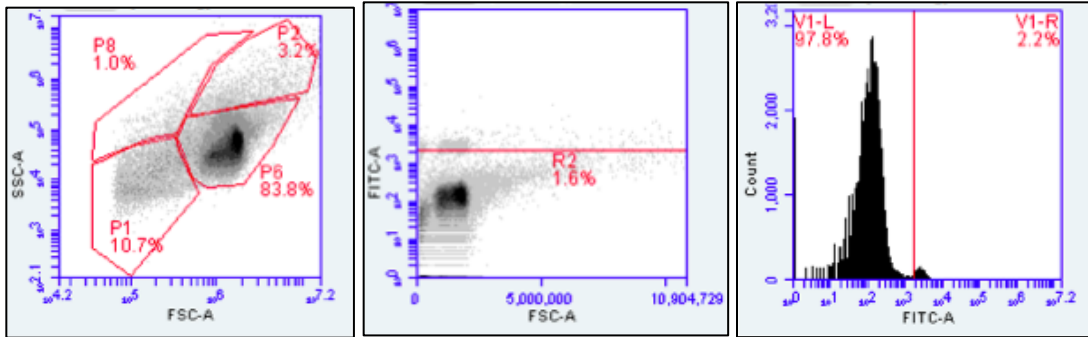


Figure 7. FITC-labeled RBC found in the pellet of a RBC mixture. Flow cytometer data for the pellet of a mixture of FITC-labeled RBC and unlabeled RBC.

Fluorescence and light microscopy of isolated cells

To confirm that the microbubbles were attaching directly to the FITC-labeled RBC, microscopy was used to view the isolated top layer of the solution of immuno-microbubbles with FITC-labeled RBC (Figure 8, Figure 9). When viewing the top layer of the sample under the light microscope, microbubbles can be seen directly adjacent to the RBC (Figure 8). The microbubbles appear as dark spots under the light field, while the RBC, due to their relatively thin center, appear lighter. It is possible that a single microbubble can link to multiple RBC (Figure 8b), or that multiple microbubbles can link to a single RBC (Figure 8c).

Using immuno-microbubbles with DiD containing lipids, along with FITC-labeled RBC, fluorescence filters could be used to visualize the colocalization of the two (Figure 9). The microbubble signal was far more disperse, due to the ratio of immuno-microbubbles, however, all RBC could be seen surrounded by microbubbles in the overlay of the two filters (Figure 9D).

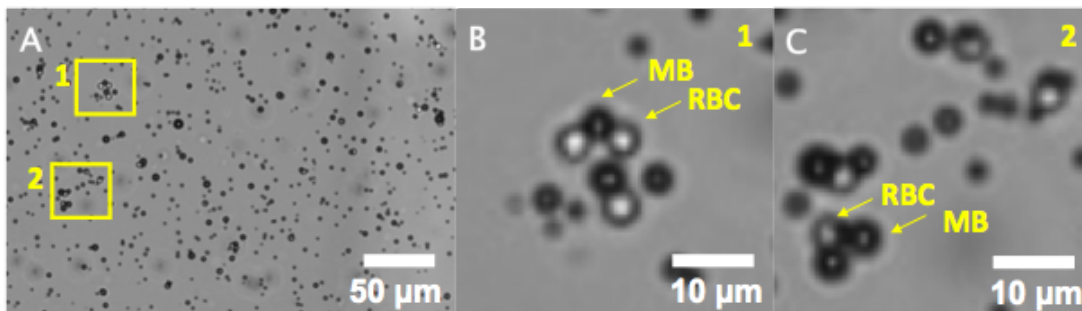


Figure 8. Light microscopy of immuno-microbubbles linking to FITC-labeled RBC. The top layer of a mixture of FITC-labeled RBC and immuno-microbubbles. **(A)** Broad view of the mixture. **(B)** Region 1, highlighted in panel A to observe linkage of one microbubble to multiple RBC. **(C)** Region 2, highlighted in A to observe multiple microbubbles linked to one RBC.

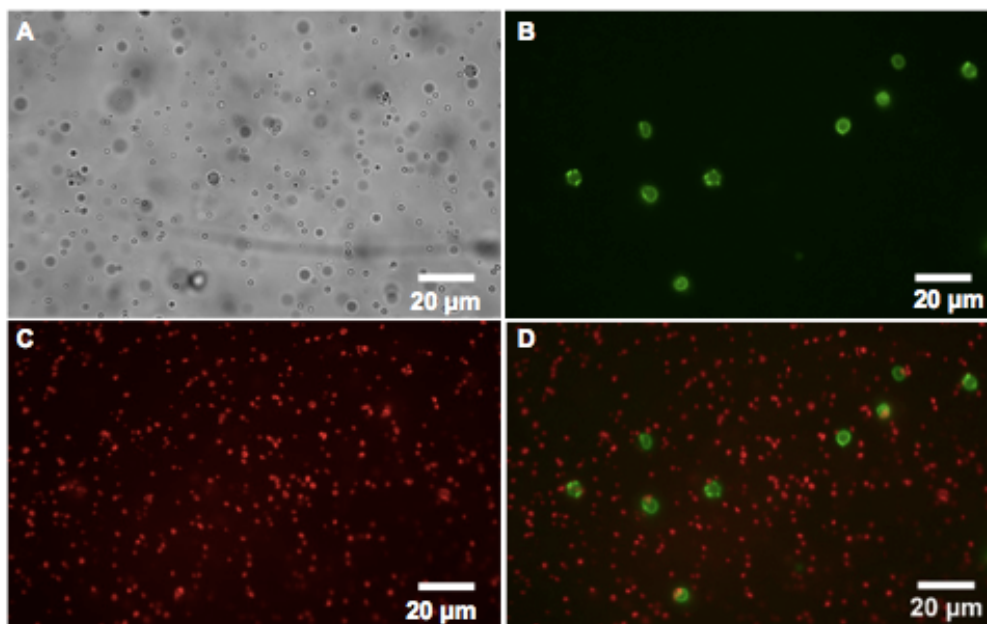


Figure 9. Fluorescence imaging of immuno-microbubbles linking to FITC-labeled RBC. **(A)** Light field image of the top layer of a mixture of immuno-microbubbles with FITC-labeled RBC. **(B)** FITC fluorescence of the cells seen in a to visualize the labeled RBC. **(C)** DiD fluorescence imaging of A to visualize microbubbles. **(D)** Overlay of figures B and C to determine microbubble linkage to RBC.

Discussion

The capture of CTCs stands to provide immense clinical benefit, as we may be able to use them to answer crucial questions, such as why cancer cells metastasize, or how MET is able to occur. Additionally, they can give diagnostic and prognostic insights into an individual's cancer and guide personalized medical approaches. CTCs also represent the most dangerous population of tumor cells, as metastasis is responsible for a majority of deaths from cancer.

The overall goal of these experiments was to develop a system capable of quickly and efficiently isolate CTCs by taking advantage of the physical properties of microbubbles. The system presented throughout this study has successfully demonstrated the use of immuno-microbubbles to rescue labeled red blood cells from populations of unlabeled red blood cells, which may indicate future success in using this system to capture CTCs from blood samples. The successful formulation of immuno-microbubbles, created by conjugation of thiolated antibodies to the surface of microbubbles formulated to include lipids with maleimide groups extending outward from the surface to allow for thioether linkage, could be observed using flow cytometry. The optimization of this system was demonstrated by varying the centrifugation conditions, as well as attempting to alter the size of the microbubbles used, which resulted in a system that ultimately demonstrated moderate enrichment of FITC-labeled RBC from the population. Finally, a change in the method of measurement provided a more accurate way to count the cells that were rescued, demonstrating a high percentage of FITC-labeled RBC from the larger population of cells. The proof that this system can in fact result in RBC floating from

linkage to buoyant immuno-microbubbles can be seen through microscopy images of the two together.

As demonstrated in Figure 1, a large percentage of microbubbles in a given formulation could be made into immuno-microbubbles through the thioether linkage proposed. These microbubbles, only when presented with a secondary IgG containing FITC, displayed a shift in fluorescence consistent with FITC fluorescence. These data imply that the linkage to the microbubbles was successful. As noted previously, the amount of microbubbles that could be recovered during the conjugation process was somewhat less than the amount input, as could be seen in the P3 ROI of Figure 1. This was presumably because the transfer of microbubbles throughout the conjugation steps resulted in a loss of microbubbles. However, the number of microbubbles that survived the conjugation process remained significantly above the amount needed for experimentation.

Once it was demonstrated that immuno-microbubbles could be easily created for experimentation, the optimization of the system was able to be commenced. It seemed best to optimize this system using RBC rather CTCs for various reasons. Perhaps the most obvious of these reasons is that CTCs are rather difficult to acquire, which remains the purpose of developing this system to begin with. However, one could argue that the use of immortalized cells could have mimicked much of what would be observed in CTCs. While immortalized cells certainly share similarities with CTCs, the biomarkers that would be targeted using the immuno-microbubble system will likely not be present regardless of the use of immortalized cells or RBC. Additionally, RBC are much easier to

acquire and label than immortalized cells in these experiments, which make RBC a more logical starting point for experimentation.

To begin the optimization process, centrifugation conditions were first analyzed. Though, in theory, the separation of immuno-microbubble linked cells from those not linked could have been achieved simply by waiting, since RBC will naturally fall to the bottom of solution and microbubbles will naturally rise, centrifugation seemed necessary for the sake of time. Centrifugation would pellet all cells at the bottom, while those linked to the immuno-microbubbles would be able to escape this pellet and float. Some concerns with this approach included the idea that centrifugation is too gentle may not successfully pellet the cells and that centrifugation that is too harsh could damage the cells. The first of these problems was addressed in Figure 2 and Figure 3. These figures assessed the background RBC that could be collected from the top layer of solution without the presence of microbubbles. If all RBC were pelleted, no RBC should be detected from flow cytometry of the top layer of solution. After centrifugation of 8 minutes at 100 x g, nearly all RBC were pelleted at the bottom of the tube.

Some other concerns about this methodology include the potential of centrifugation to disrupt the linkage of the microbubbles to the cells and the stability of the microbubbles during centrifugation. Given the strength of the affinity of the antibody on the immuno-microbubbles for the FITC on the RBC surface, it is highly unlikely that this linkage would be disrupted by such weak centrifugation. Other immuno-microbubbles have reported extremely high binding-efficiencies, which makes this an un concerning possibility (Wang et al., 2018). Additionally, the stability of the

microbubbles during centrifugation has been assessed numerous times and microbubbles have been found to withstand greater than 400 x g without significant loss of microbubbles, providing support that 100 x g will not cause damage to the microbubble population (Owen et al., 2018).

Once the centrifugation conditions were optimized, the system was implemented for initial testing (Figure 4). The resulting recovery rate of FITC-labeled RBC was around 39.5%, which seems relatively low, given the incredibly small number of CTCs that would be present in the blood. However, this number must be put into perspective by comparing it to known methods of CTC isolation. The highest reported recovery rate of CTCs by the current gold standard of CTC isolation, CellSearch, sits at around 61%, with other methods of isolation performing much closer to 40% (Maertens et al., 2017). This implies that the recovery of labeled cells is on par with other forms of CTC isolation. It is yet to be seen if this same recovery rate can be achieved using actual CTCs.

Furthermore, as was briefly mentioned earlier, the mechanism by which the flow cytometer counts cells is not ideal for the experimental system presented. This is because the probe through which the flow cytometer collected the sample reaches to the bottom of the sample tube. The microbubbles rapidly float to the top of the sample, carrying along with them the FITC-labeled RBCs that are supposed to be quantified. This may prevent the flow cytometer from accurately counting the cells that are within the sample, despite the fact that those cells have, in fact, been released from the cell pellet by the immuno-microbubbles. An attempt was made to correct for this by shaking the sample to mix the solution just prior to measurement, though that was by no means a perfect solution.

Because of this flaw with the quantification method, it is very likely that the recovery rate was much higher than what was presented in Figure 4.

In order to improve the recovery rate further, it was hypothesized that an increase in microbubble size would correlate to an increase in buoyant force and thus increase the number of cells that could be floated from the cell pellet. If the cells that were not collected from the experiments in Figure 4 were not recorded because they were linked to microbubbles but remained stuck in the pellet, this greater buoyant force should improve the recovery rate. As is apparent from Figure 6, this did not seem to be the case. There was no apparent difference from the use of larger microbubbles, even though there was a demonstrable increase in the average size of the microbubble population (Figure 5). There are several reasons why these observations may have occurred. The first is that any RBC not rescued in these experiments were not recovered simply because no immuno-microbubbles targeted the RBC, which would render bubble size irrelevant. It is also possible that the increase in size was not enough to free cells that were pelleted at the bottom. Further experiments with even larger microbubbles would have to be used to test this.

Ultimately, this system will be used to isolate CTCs from whole blood samples, without any purification steps. Therefore, it was necessary to test if this system could isolate a subpopulation of cells from a larger population. To prove that immuno-microbubbles could achieve this goal, immuno-microbubbles were used to target a population of FITC-labeled RBC and remove them from a much larger population of unlabeled RBC. To account for the issues with measurement using the flow cytometer,

the measurement came from the pellet rather than the top layer of the sample.

Theoretically, all FITC-labeled RBC that are not found in the pellet should have floated out of it. While this is by no means a perfect system for quantification, it does provide a seemingly more accurate way to quantify the cells. Using this methodology, it was determined that around 72% of cells were able to be removed from the pellet (Figure 7). This number far surpasses the recovery rate recorded for the CellSearch technique, implying that the use of immuno-microbubbles may be superior to the current method of CTC isolation. It is likely that some of the FITC-labeled RBC that were not found in the pellet simply had not pelleted, despite not being linked to any immuno-microbubbles, falsely inflating the number calculated for recovery rate. However, as demonstrated in Figure 2 and Figure 3, the number of cells not pelleted was likely very low, given that the centrifugation conditions seemed to pellet nearly all RBC.

In order to confirm that the system was functioning as proposed, microscopy images were taken to directly observe the linkage between the immuno-microbubbles and the RBC. As highlighted in Figure 8, the linkage appeared successful based on the proximity of the immuno-microbubbles to the RBC. Further fluorescence imaging further confirmed that the RBC were surrounded by microbubbles (Figure 9). Far more microbubbles were present than RBC, so it is possible that the localization of the two in Figure 9 could be from random chance, though this is unlikely given the successful recovery rates observed in prior experiments.

Overall, the results of these experiments suggest that using immuno-microbubbles to enrich a subpopulation of cells through buoyant force is a promising, novel technique.

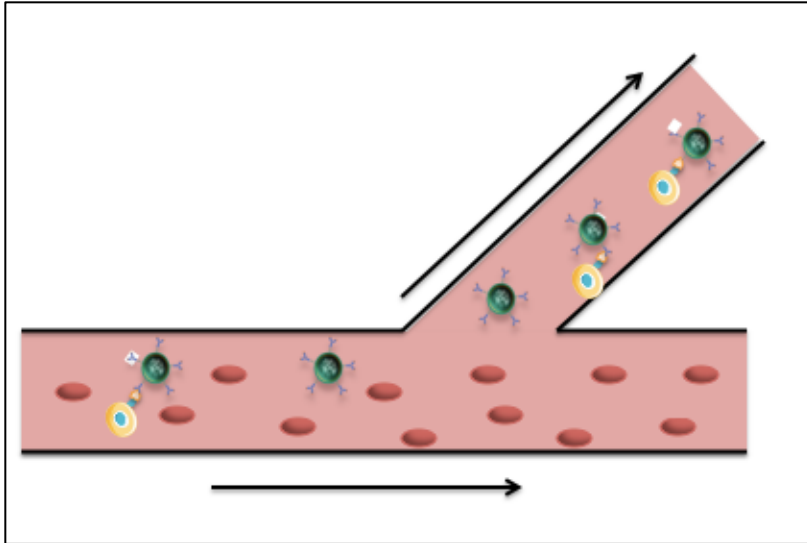
The recovery rates observed demonstrate comparable, or even superior percentages compared to current methods of cell isolation. Additionally, the cost of these experiments is far below what would be necessary to perform techniques, such as CellSearch, which require the use of kits that can cost thousands of dollars, while also necessitating a CellSearch system which can cost over \$100,000. In contrast, the only required materials for the system proposed here are the materials to formulate microbubbles and the antibodies to which the microbubbles will be conjugated.

There are a large number of ways that this research can be expanded to prove the efficacy of this system for CTC isolation for use in liquid biopsy. The most obvious next step would be to test the ability of immuno-microbubbles to capture cancer cells from whole blood samples. One would predict that the system would function much the same, although a few difference between cancer cells and RBC may cause some differences. For instance, cancer cells possess much greater mass compared to RBC. This would have an impact on the amount of buoyant force necessary to float the cancer cells within solution. On the other hand, cancer cells also have a greater surface area, which may create more space for microbubble linkage, therefore compensating for this increase in necessary buoyant force. Another difference lies in the biomarkers that would be present. Cancer cells are notoriously heterogenous, which could make the production of immuno-microbubbles specific for CTCs somewhat difficult. As mentioned earlier, the EpCAM biomarker may prove an efficient target for its role in EMT, though even this marker is not present on 100% of CTCs. It may be possible to compensate for this by coating the surface of the microbubbles with multiple antibodies specific to other common

biomarkers. This is another variable that requires exploration before this system of CTC isolation can be ready for use.

Some other tests that may provide insights into the viability of using immuno-microbubbles for rare cell isolation would be to perform animal tests. By injecting a limited number of labeled cells into the circulatory system of a rat and allowing circulation before taking a blood sample. If immuno-microbubbles are able to isolate those same labeled cells from a whole blood sample from an animal in this scenario, it would provide strong support for the use of this system in human trials.

In order to improve the system further, it would also be possible to create microfluidic devices for cell sorting based on buoyancy. Microfluidic devices have been developed for microbubbles currently, but are not in use for cell sorting (Lin et al., 2016). The basic premise of such a device would be that blood samples mixed with immuno-microbubbles are flowed through a network where cells will remain within a specified path unless they possess a buoyancy that will carry them up another path (Model 5).



Model 5. Microfluidic device to sort cells based on buoyancy from immuno-microbubble linkage.

In summary, the data presented from these studies provides a framework for the use of immuno-microbubbles to be used for rare CTC isolation. This novel method of CTC isolation stands to both improve the costs associated with liquid biopsies of cancer patients, as well improve the overall effectiveness of these tests. Given the value of using CTCs to determine prognosis and personalized medical approaches to treatment of cancers, it is crucial that improvements be made to the current methods of CTC isolation. Further testing will be necessary to establish the exact efficacy of the proposed system to isolate cancerous cells, rather than RBC, but there is reason to believe that those tests will ultimately be successful. Hopefully, using immuno-microbubbles to isolate CTCs from whole blood samples from cancer patients can be developed into a new gold standard technique.

References

- Aceto, N; Bardia, A; Miyamoto, DT; Donaldson, MC; Wittner, BS; Spencer, JA; Yu, M; Pely, A; Engstrom, a; Zhu, H; Brannigan, BW; Kapur, R; Scott, SL; Shioda, T; Ramaswamy, S; Ting, DT; Lin, CP; Toner, M Haber, DA; Maheswaran, S. Circulating tumor cell clusters are oligoclonal precursors of breast cancer metastasis: *Cell* **2014** 158(5), 1110-1122.
- Alnemri, ES; Livingston, DJ; Nicholson, DW; Salveson, G; Thornberry, NA; Wong, WW; Yuan, J. Human ICE/CED-3 protease nomenclature: *Cell* **1996** 87(2), 171.
- American Cancer Society. Facts and figures 2019: US cancer death rate has dropped 27% in 25 years. **2019**
- American Cancer Society. Known and probable human carcinogens. **2016**
- Baccelli, I; Schneeweiss, A; Riethdorf, S; Stenzinger, A; Schillert, A; Vogel, V; Klein, C; Saini, M; Bäuerle, T; Wallwiener, M; Holland-Letz, T; Höfner, T; Sprick, M; Scharpf, M; Marmé, F; Peter Sinn, H; Pantel, K; Weichert, W; Trumpp, A. Identification of a population of blood circulating tumor cells from breast cancer patients that initiates metastasis in a xenograft assay: *Nature Biotechnol* **2013** 31, 539-544.
- Borden, MA; Kruse, DE; Caskey, CF; Zhao, S; Dayton, PA; Ferrera, KW. Influence of lipid shell physicochemical properties on ultrasound-induced microbubble destruction: *IEEE T Ultrason Ferr* **2005** 52(11), 1992-2002.
- Cancer Research UK. Health economics: the cancer drug cost conundrum. **2016**

- Carpentier, A; Canney, M; Vignot, A; Reina, V; Beccaria, K; Horodyckid, C; Karachi, C; Leclercq, D; Chapelon, JY; Capella, L; Cornu, P; Sanson, M; Hoang-Xuan, K; Delattre, JY; Idbah, A. Clinical trial of blood-brain barrier disruption by pulsed ultrasound: *Sci Transl Med* **2016** 343(8), DOI: 10.1126/scitranslmed.aaf6086.
- CellSearch Circulating Tumor Cell Test. Benefits of CellSearch CTC test. **2019**
- Centers for Disease Control and Prevention. Family history and cancer. **2018**
- Chen, Y; Zhao, Z; Chen, Y; Lv, Z; Ding, X; Wang, R; Xiao, H; Hou, C; Shen, B; Feng, J; Guo, R; Li, Y, Peng, H; Han, G; Chen, G. An epithelial-to-mesenchymal transition-inducing potential of granulocyte macrophage colony-stimulating factor in colon cancer: *Sci Rep* **2017** 7, 8265.
- Dagogo-Jack, I; Shaw, AT. Tumor heterogeneity and resistance to cancer therapies: *Nat Rev Clin Oncol* **2018** 15, 81-94.
- D'arrigo, J. Stable gas-in-liquid emulsions: *Elsevier Science* **2011** 19(1).
- DeBerardinis, RJ; Lum, JJ; Hatzivassiliou, G; Thompson, CB. The biology of cancer: metabolic reprogramming fuels cell growth and proliferation: *Cell Metab* **2008** 7(10), 11-20.
- Feshitan, JA; Chen, CC; Kwan, JJ; Borden, MA. Microbubble size isolation by differential centrifugation: *J Colloid Interface Sci* **2009** 329(2), 316-324.
- Haber, DA; Velculescu, VE. Blood-based analysis of cancer: circulating tumor cells and circulating tumor DNA: *Cancer Discov* **2014** 4(6), 650-661.
- Hanahan, D; Folkman, J. Patterns and emerging mechanisms of the angiogenic switch during tumorigenesis. *Cell* **1996** 86(3), 353-364.

- Hanahan, D; Weinberg, RA. The hallmarks of cancer: *Cell* **2000** 100(1), 57-70.
- Hanahan, D; Weinberg, RA. The hallmarks of cancer: The next generation: *Cell* **2011** 144(5), 646-674.
- Harding, C; Pompei, F; Wilson, R. Peak and decline in cancer incidence, mortality and prevalence at old ages: *Cancer* **2012** 118(5), 1371-1386.
- Hosokawa, M; Kenmotsu, H; Koh, Y; Yoshino, T; Yoshikawa, T; Naito, T; Takahashi, T; Murakami, H; Nakamura, Y; Tsuya, A; Shukuya, T; Ono, A; Akamatsu, H; Watanabe, R; Ono, S; Mori, K; Kanbara, H; Yamaguchi, K; Tanaka, T; Matsunaga, T; Yamamoto, N. Size-based isolation of circulating tumor cells in lung cancer patients using a microcavity array system: *PLoS One* **2013** 8(6), e67466.
- Huang, S; Shao, K; Liu, Y; Kuang, Y; An, S; Guo, Y; Ma, H; Jiang, C. Tumor-targeting and microenvironment-responsive smart nanoparticles for combination therapy of antiangiogenesis and apoptosis: *ACS Nano* **2013** 7, 2860-2871.
- Jaiswal, S; Jamieson, CH; Pang, WW; Park, CY; Chao, MP; Majeti, R; Traver, D; van Rooijen, N; Weissman, IL. CD47 is upregulated on circulating hematopoietic stem cells and leukemia cells to avoid phagocytosis: *Cell* **2009** 138(2), 271-285.
- Karabacak, NM; Spuhler, PS; Fachin, F; Lim, EJ; Pai, V; Ozkumur, E; Martel, JM; Kojic, N; Smith, K; Chen, P; Yang, J; Hwang, H; Morgan, B; Trautwein, J; Barber, TA; Scott, SL; Maheswaran, S; Kapur, R; Haber, DA; Toner, M. Microfluidic, marker-free isolation of circulating tumor cells from blood samples: *Nature Prot* **2014** 9, 694-710.

- Kelly, LA. Liposome drug delivery systems. US4356167A. **1981**
- Kermanshah, L; Poudineh, M; Ahmed, S; Nguyen, LNM; Srikant, S; Makonnen, R; Cantu, FP; Corrigan, M; Kelley, SO. Dynamic CTC phenotypes in metastatic prostate cancer models visualized using magnetic ranking cytometry: *RSC* **2018** 18, 2055-2064.
- Krebs, MG; Hou, JM; Ward, TH; Blackhall, FJ. Circulating tumor cells: their utility in cancer management and predicting outcomes: *Ther Adv Med Oncol* **2010** 2(6), 351-361.
- Li, Q; Damish, AW; Frazier, Z; Liu, D; Reznichenko, E; Kamburov, A; Bell, A; Zhao, H; Jordan, EJ; Gao, SP; Ma, J; Abbosh, PH; Bellmunt, J; Pillmack, ER; Lazaro, JB; Solit, DB; Bajorin, D; Rosenberg, JE; D'Andrea, AD; Riaz, N; Van Allen, EM; Iyer, G; Mouw, KW. *ERCC2* helicase domain mutations confer nucleotide repair deficiency and drive cisplatin sensitivity in muscle-invasive bladder cancer: *Clin Cancer Res* **2019** 25(3), 10.1158/1078-0432.CCR-18-1001.
- Lin, H; Chen, J; Chen, C. A novel technology: microfluidic devices for microbubble contrast agent generation: *Med Biol Eng Comput* **2016** 54(9), 1317-1330.
- Lipsman, N; Meng, Y; Bethune, AJ; Huang, Y; Lam, B; Masellis, M; Herrmann, N; Heyn, C; Aubert, I; Boutet, A; Smith, GS; Hynynen, K; Black, SE. Blood-brain barrier opening in Alzheimer's disease using MR-guided focused ultrasound: *Nature Comm* **2018** 9, 2336.
- Lux, J; Vezeridis, AM; Hoyt, K; Adams, SR; Armstrong, AM; Sirsi, SR; Mattrey, RF. Thrombin-activatable microbubbles as potential ultrasound contrast agents for the

detection of acute thrombosis: *ACS Appl Mater Interfaces* **2017** 9(43), 37587-37596.

Maertens, Y; Humberg, V; Erlmeier, F; Steffens, S; Steinestel, J; Bogemann, M; Jan Schrader, A; Bernemann, C. Comparison of isolation platforms for detection of circulating renal cell carcinoma cells: *Oncotarget* **2017** 8(50), 87710-87717.

Markiewicz, A; Ksiazkiewicz, M; Welnicka-Jasckiewicz, M; Seroczynska, B; Skokowski, J; Szade, J; Zaczek, AJ. Mesenchymal phenotype of CTC-enriched blood fraction and lymph node metastasis formation potential: *PLoS* **2014** doi.org/10.1371/journal.pone.0093901.

Muller, V; Riethdorf, S; Rack, B; Janni, W; Fasching, PA; Solomayer, E; Aktas, B; Kasimir-Bauer, S; Pantel, K; Fehm, T. Prognostic impact of circulating tumor cells assessed with the CellSearch system AdnaTest Breast in metastatic breast cancer patients: the DETECT study: *Breast Cancer Res* **2012** 14, R118.

Narihira, K; Watanabe, A; Sheng, H; Endo, H; Feril, LB; Irie, Y; Ogawa, K; Moosavi-Nejad, S; Kondo, S; Kikuta, T; Tachibana, K. Enhanced cell killing and apoptosis of oral squamous cell carcinoma cells with ultrasound in combination with cetuximab coated albumin microbubbles: *J Drug Target* **2017** 26(3), 278-288.

National Cancer Institute. Age and cancer risk. **2015**

National Cancer Institute. Cancer statistics. **2018a**

National Cancer Institute. List of Cancer Drugs. **2019**

National Cancer Institute. The challenging landscape of cancer and aging: charting a way forward. **2018b**

- National Cancer Institute. Tumor DNA sequencing in cancer treatment. **2017**
- O'Reilly, MA; Hynynen, K. Ultrasound and microbubble-mediated blood-brain barrier disruption for targeted drug delivery of therapeutics to the brain: *JTDD* **2018** 1831, 111-119.
- Owen, J; Crake, C; Lee, JY; Carugo, D; Beguin, E; Khrapitchev, AA; Browning, RJ; Sibson, N; Stride, E. A versatile method for preparation of particle-loaded microbubbles for multimodality imaging and targeted drug delivery: *Drug Deliv Transl Res* **2018** 8(2), 342-356.
- Park, SJ; Weng, JG; Tien, CL. A molecular dynamics study on the surface tension of microbubbles: *Int J Heat Mass Trans* **2001** 44(10), 1849-1856.
- Pederson, JK; Engholm, G; Skytthe, A; Christensen, K. Cancer and aging: epidemiology and methodological challenges: *Acta Oncol* **2016** 55, 7-12.
- Pray, L. DNA replication and causes of mutation: *Nature Education* **2008** 1(1), 214.
- Preston, BD; Albertson, TM; Herr, AJ. DNA replication fidelity and cancer: *Semin Cancer Biol* **2010** 20(5), 281-293.
- Reiter, RE; Gu, Z; Watabe, T; Thomas, G; Szigeti, K; Davis, E; Wahl, M; Nisitani, S; Yamashiro, J; Le Beau, MM; Loda, M; Witte, ON. Prostate cell antigen: a cell surface marker overexpressed in cancer: *PNAS* **1998** 95(4), 1735-1740.
- Roser, M. Life Expectancy: *Our World in Data* **2019**
- Roovers, S; Segers, T; Lajoinie, G; Deprez, J; Versluis, M; De Smedt, SC; Lentacker, I. The role of ultrasound-driven microbubble dynamics in drug delivery: from

microbubble fundamentals to clinical translation: *ACS Langmuir* **2019** DOI:
10.1021/acs.langmuir.8b03779.

Ruhul Amin, ARM; Karpowicz, PA; Carey, TE; Arbiser, J; Nahta, R; Chen, ZG; Dong, JT; Kucuk, O; Khan, GN; Huang, GS; Mi, S; Lee, HY; Reichrath, J; Honoki, K; Georgakilas, AG; Amedei, A; Amin, A; Helferich, B; Boosani, CS; Ciriolo, MR; Chen, S; Mohammed, SI; Azmi, AS; Keith, WM; Bhakta, D; Halicka, D; Nicolai, E; Fujii, H; Aquilano, K; Ashraf, SS; Nowsheen, S; Yang, X; Bilsland, A; Shin, DM. Evasion of anti-growth signaling: a key step in tumorigenesis and potential target for treatment prophylaxis by natural compounds: *Semin Cancer Biol* **2015** 35, S55-S77.

Sartor, O; de Bono, JS. Metastatic prostate cancer: *N Engl J Med* **2018** 378, 645-657.

Schwab, M. Self-sufficiency in growth signals. In: *Encyclopedia of Cancer* **2011**
Springer, Berlin, Heidelberg.

Seyfried, TN; Huysentruyt, LC. On the origin of cancer metastasis: *Crit Rev Oncog* **2013**
18(1-2), 43-73.

Sirsi, S; Borden, M. Microbubble compositions, properties and biomedical applications:
Bubble Sci Eng Technol **2009** 1(1-2), 3-17.

Soubrier, C; Liao, PJ; Ricketts, CJ; Wei, D; Yang, Y; Baranes, SM; Gibbs, BK; Ohanjanian, L; Krane, LS; Scroggins, BT; Killian, JK; Wei, MH; Kijima, T; Meltzer, PS; Citrin, DE; Neckers, L; Vocke, CD; Linehan, WM. Targeting loss of Hippo signaling pathway in *NF-2* deficient papillary kidney cancers: *Oncotarget* **2018** 9(12), 10723-10733.

- Sulli, G; Rommel, A; Wang, X; Kolar, MJ; Puca, F; Saghatelian, A; Plikus, MV; Verma, IM; Pansa, S. Pharmacological activation of REV-ERBs is lethal in cancer and oncogene-induced senescence: *Nature* **2018** 553, 352-355.
- Tan, GJ; Peng, ZK; Lu, JP; Tang, FQ. Cathepsins mediate tumor metastasis: *World J Biol Chem* **2013** 4(4), 91-101.
- Tauriello, DVF; Polomo-Ponce, S; Stork, D; Berenguer-Llergo, A; Badia-Ramentol, J; Iglesias, M; Sevillano, M; Iliza, S; Canellas, A; Hernando-Momblona, X; Byrom, D; Matarin, JA; Calon, A; Rivas, EI; Nebreda, AR; Riera, A; Attolini, CSO; Batlle, E. TGF β drives immune evasion in genetically reconstituted colon cancer metastasis: *Nature* **2018** 554, 538-543.
- Theodoropoulos, PA; Polioudaki, H; Agelaki, S; Kallergi, G; Saridaki, Z; Mavroudis, D; Georgoulas, V. Circulating tumor cells with a putative stem cell phenotype in peripheral blood of patients with breast cancer: *Cancer Lett* **2010** 288(1), 99-106.
- Ting, DT; Wittner, BS; Ligorio, M; Jordan, NV; Shah, AM; Miyamoto, DT; Aceto, N; Bersani, F; Brannigan, BW; Xega, K; Ciciliano, JC; Zhu, H; MacKenzie, OC; Trautwein, J; Arora, KS; Shahid, M; Ellis, HL; Qu, N; Bardeesy, N; Rivera, MN; Deshpande, V; Ferrone, CR; Kapur, R; Ramaswamy, S; Shioda, T; Toner, M; Maheswaran, S; Haber, DA. Single-cell RNA sequencing identifies extracellular matrix gene expression by pancreatic circulating tumor cells: *Cell Rep* **2014** 8(6), 1905-1918.
- Tu, J; Zhang, H; Yu, J; Liufu, C; Chen, Z. Ultrasound-mediated microbubble destruction: a new method in cancer immunotherapy: *Onco Targets Ther* **2018** 11, 5763-5775.

- Unnikrishnan, S; Du, Z; Diakova, GB; Klibanov, AL. Formation of microbubbles for targeted ultrasound contrast imaging: practical translation considerations: *ACS Langmuir* **2018** DOI: 10.1021/acs.langmuir.8b03551.
- Wang, FB; Yang, XQ; Yang, S; Wang, BC; Feng, MH; Tu, JC. A higher number of circulating tumor cells (CTC) in peripheral blood indicates poor prognosis in prostate cancer patients- a meta-analysis: *Asian Pas J Cancer Prev* **2011** 12, 2629-2635.
- Wang, G; Benasutti, H; Jones, JF; Shi, G; Benchimol, M; Pingle, S; Kesari, S; Yeh, Y; Hsieh, LE; Liu, YT; Elias, A; Simberg, D. Isolation of breast cancer CTCs with multitargeted buoyant immunobubbles: *Colloids Surf B Biointerfaces* **2018** 161, 200-209.
- Wang, L; Balasubramanian, P; Chen, A; Kummar, S; Evrard, YA; Kinders, R. Promise and limits of CellSearch platform for evaluating pharmacodynamics in circulating tumor cells (CTC): *Semin Oncol* **2017** 43(4), 464-475.
- Wright, WE; Pereira-Smith, OM; Shay, JW. Reversible cellular senescence: implications for immortalization of normal human diploid fibroblasts: *Mol Cell Biol* **1989** 9(7), 3088-3092.
- Ye, X; Brabletz, T; Kang, Y; Longmore, GD; Nieto, MA; Stanger, BZ; Yang, J; Weinberg, RA. Upholding a role for EMT in breast cancer metastasis: *Nature* **2017** 547, E1-E3.

- Zhang, C; Moore, LM; Li, X; Alfred Young, WK; Zhang, W. IDH1/2 mutations target a key hallmark of cancer by deregulating cellular metabolism in glioma: *Neuro Oncol* **2013** 15(9), 1114-1126.
- Zhang, J; Chen, K; Fan, ZH. Circulating tumor cell isolation and analysis: *Adv Clin Chem* **2017** 75, 1-31 doi: 10.1016/bs.acc.2016.03.003.
- Zhang, X; Zhou, J; Zhang, C; Zhang, D; Su, X. Rapid detection of *Enterobacter cloacae* by immunomagnetic separation and colloidal gold-based immunochromatographic assay: *RSC* **2016** 6, 1279-1287.
- Zhu, S; Qing, T; Zheng, Y; Jin, L; Shi, L. Advances in single-cell RNA sequencing and its application in cancer research: *Oncotarget* **2017** 8(32), 53763-53779.